UNIVERSITY OF OKLAHOMA

GRADUATE COLLEGE

INFLUENCE OF COMPACTION AND QUALITY CONTROL ON THE PERFORMANCE OF GRS-IBS BRIDGE ABUTMENTS

A THESIS

SUBMITTED TO THE GRADUATE FACULTY

in partial fulfillment of the requirements for the

Degree of

MASTER OF SCIENCE

By

JÉRÔME BOUTIN
Norman, Oklahoma
2020

INFLUENCE OF COMPACTION AND QUALITY CONTROL ON THE PERFORMANCE OF GRS-IBS BRIDGE ABUTMENTS

A THESIS APPROVED FOR THE
SCHOOL OF CIVIL ENGINEERING AND ENVIRONMENTAL SCIENCE

BY THE COMMITTEE CONSISTING OF

Dr. Kianoosh Hatami, Chair

Dr. Amy Cerato

Dr. Gerald Miller

ACKNOWLEDGEMENTS

I would like to express my sincere gratitude to my academic advisor, Dr. Kianoosh Hatami, who helped me throughout my time at the University of Oklahoma. He was the first to contact me about working together on potential projects while I was still in my home university, with my admission to OU all but confirmed. He helped me choose an adequate coursework for me to learn essential materials about the field I wanted to have my career in. During my thesis work, he managed to guide and mentor me while still giving me the space to question myself about the purpose of some of the tasks I was doing. Thanks to his knowledge in a wide array of topics, I managed to learn a lot just from discussing with him about the various intricacies of this study. With him being always available and ready to accommodate our needs in the shortest delays, this study could not have gone this far without him.

I would like to thank the committee members, Dr. Amy Cerato and Dr. Gerald Miller, for taking the time to review this thesis. Their feedback was essential in ensuring the quality of this study. I would also like to thank my home university advisor, Mr. Claude Bacconnet, for always checking up on me and asking me about my coursework and thesis progress.

I would like to thank Ph.D. candidate Ridvan Doger, who was working on this project before I came along. He made sure to explain everything to me about the test station and its components to make sure that I could confidently take the lead on the project without being overwhelmed. He also always was ready to help and answer in the shortest delays any of my questions despite working as a full-time engineer.

I would like to express my gratitude to the Fears Laboratory manager, Michael Schmitz, for always being available and ready to help throughout the study. His knowledge and experience allowed the construction and testing phases of the models to go smoothly. If it were not for him, there is no doubt that this study would have taken longer to complete.

And last but not least, I would like to thank all my colleagues who helped me greatly during this study: Stephen Schnabel, Kirby Falcon, Connor Jones, Alyssa Weishaar, Daniel Farley, Emma Bachman, Miguel Payan, Javier Alejandro and Tareq Abuawad.

Table of Contents

List of Tables

List of Figures

ABSTRACT

GRS-IBS is a type of bridge abutment that has become more widespread in local and county roads across the United States due to its demonstrated advantages including expedited construction at reduced costs and prevention of the bump-at-end-of-the-bridge problem. Over the last two decades, guidelines have been developed to help with the analysis and design of GRS-IBS. However, influences that factors such as the choice of backfill, and compaction effort could have on the stability and performance of GRS abutments have not been investigated in detail. In this study, three instrumented, full-scale (i.e. 8 ft-tall) model GRS abutments were constructed in an outdoor test facility at the University of Oklahoma to investigate their construction and load-bearing performance as a function of backfill gradation and compaction. These model abutments were part of a longer-term study where influences that other design parameters (including the choice of facing and reinforcement spacing) could have on GRS abutment construction and load-bearing performance have been investigated.

The models in this study were built with CMU blocks for their facing and a woven geotextile for reinforcement, which were placed in the compacted backfill at 8-inch vertical spacing. The backfill type investigated included both an open-graded and a dense-graded aggregate in alternative abutment models. All the component materials used in the models either met or were comparable to the specifications in the Federal Highway Administration's (FHWA) latest guidelines. The test results from this study were compared with those from a control abutment model with a reduced compaction effort from a recent study by the same research group at OU.

Results of the study indicated significant improvements in the load-bearing capacity and performance of GRS abutments in models with increased compaction effort, consistent with FHWA recommendations. The load-settlement responses of all three abutment models exceeded minimum FHWA requirements by significant margins. It was found that all models could carry

surcharge loads of an order of magnitude greater than the FHWA service load of 4 ksf (i.e. 40 ksf) with no more than a maximum of 1.4 inches of settlement at the loading beam simulating the bridge seat. Additionally, facing lateral deformations at the maximum 40 ksf surcharge load level applied to the models were found to be merely 0.25 in, which is nearly half of the limiting value in FHWA guidelines at the significantly smaller load of 4 ksf. Reinforcement strains and axial loads, as calculated from wire potentiometer readings, did not exceed 1.8% and 1,235 lb/ft, respectively. The dense-graded fill showed some improvement over open-graded aggregate, albeit at the expense of significantly longer construction time due to the more challenging compaction procedure. Post-mortem survey of backfill density using the ASTM sand cone method showed that using three compaction passes per lift had resulted in unit weights that well exceeded the required 95% compaction level for GRS abutments in FHWA guidelines.

Chapter 1 – INTRODUCTION

1.1 Background on GRS-IBS

Geosynthetic Reinforced Soil structures (GRS) are widely used in the US and around the world in transportation and urban development projects. These composite structures are built by placing geosynthetic reinforcement layers between compacted layers of soil. The term GRS is very broad and can refer to a multitude of GRS structure types, all having different functions. Some of the most common uses of GRS structures are for retainment, supporting and stability purposes.

GRS structures used as bridge abutments are part of Geosynthetic Reinforced Soil-Integrated Bridge Systems (GRS-IBS). These are a special kind of GRS structures that are designed as shallow foundations to support the load of both the bridge deck and the overpassing traffic. GRS-IBS projects to date have shown several economic advantages over deep-foundation alternatives including shorter construction time and lower abutment costs, especially for smaller bridges in rural and county roads. They also help eliminate the problem of bump-at-end-of-bridge associated with deep-foundation abutments.

1.2 Purpose of the study

This research is the continuation of a bigger project aiming to understand the behavior of GRS-IBS structures by doing experiments on full-scale models of abutments. Three different GRS models were previously built and tested at Fears Lab. The first one, GRS#1, was built using geotextile reinforcement spaced every 8 inches, with a facing made of concrete masonry unit (CMU) blocks (8” × 8” × 16”). GRS#2 had the CMU blocks of the facing replaced with large concrete blocks (24” × 24” × 48”) with reinforcement spacing kept at 8 inches. The last one, GRS#3, was basically the same as GRS#2 with reinforcements spacing of 12 inches. For each of

those experiments, the backfill type and compaction were held constant. #2 Cover gravel was used as backfill and one pass of compaction was done using a jumping jack.

Those previous GRS experiments focused on the influence of facing type and reinforcement spacing but since the backfill compaction effort was the same for all of them, its influence could not be analyzed. The backfill compaction was not monitored either. Thus, this research project focuses on the influence of the backfill compaction and quality control on the GRS performance. To accomplish this, three new GRS models were constructed, identical to some of the previous attempts, with an emphasis put on the compaction of the backfill. The models' structural performances, among others, were then compared to each other.

1.3 Study objectives and tasks

The main objective of this research was to build new GRS models that are identical to some of the previous one and see how the increased compaction affect their structural performances. Another objective was to verify the quality of the compaction of the backfill when in place. The compaction used for all three new models was of three passes per lift, as recommended by the Federal Highway Administration (FHWA) guidelines. The performance tests helped determine if this amount of compaction is truly necessary or if it just overdesigns the structure.

To reach these objectives, several ancillary tests were carried out:

- Sieve analysis were done on the aggregates provided to verify that they correspond to the aggregate characteristics recommended by the FHWA.
- A compaction test bed was run to determine the unit weight of the gravel #2 Cover when compacted with one and three passes using the jumping jack.
- Additionally, several relative density tests were run on both gravels (#2 Cover and ODOT Type A) to obtain the range of densities of the aggregates.

- Direct Shear Tests (DST) were run to determine the strength characteristics of the gravels. These could be particularly useful in case of the creation of numerical models of GRS-IBS.

All these tasks were complementary to the main one: the construction and performance testing of three GRS models. GRS#4 and GRS#5 were complete replicas of GRS#1 with the exception that both were built using three compaction passes per lifts. GRS#4 was completely instrumented while GRS#5 was free of any instrumentation and was used as a construction time control model. GRS#6 was identical to GRS#3 but instead of using gravel #2 Cover as fill, ODOT Type A was used.

1.4 Thesis layout

This research thesis is comprised of seven chapters. The first chapter contains some background information on GRS-IBS, reasons as to why the study was needed and the tasks necessary to realize the study. The second chapter is a literature review on the different characteristics that can impact the performances of GRS-IBS. The third chapter explain the study approach as well as the different equipment used. The fourth chapter goes more in depth about the ancillary tests and tasks, as well as the results obtained from them. The fifth chapter is about the construction of the GRS-IBS models themselves, while going over the methodology used for construction, instrumentation and performance tests. The sixth chapter goes over the results and analyses that can be made from the testing and surveying of the models. The seventh and final chapter presents a summary of what can be learned from this study as well as what could be done in the future to complement the study.

Chapter 2 – LITERATURE REVIEW

This literature review discusses how the performances of GRS-IBS can be influenced by the materials used and other design related factors. The experiments that have been carried out to reach these conclusions vary from large scale test subjects, project monitoring, and creation of numerical models of GRS-IBS.

2.1 Factors influencing the performance of GRS-IBS

2.1.1 Type of backfill

The first, and largest, component of GRS-IBS is the soil backfill component. The soil backfill has an important role to play in the stability and performance of the GRS-IBS since its characteristics will alter the behavior of the entire structure.

2.1.1.1 Gradation and constitution

To prevent any issues related to the abutment, it needs to meet certain graduation and aggregate quality requirements. According to the Federal Highway Administration (FHWA) guidelines (Adams and Nicks 2018) these aggregates should be constituted of crushed and angular stone or gravel, both durable and hard. Additionally, there should be no organic or shale presence in the fill, or any material susceptible to swell or shrink because of moisture content variance. The plasticity index (PI) of the material should also be less than 6.

The gradation of the backfill can also play a role. The FHWA guidelines (Adams and Nicks 2018) on constructing GRS bridge abutments recommend that the backfill material should either be well-graded or open-graded aggregate. The number of fines (sieve #200) should be limited to less than 12 percent in case of well-graded backfill and as close to 0 percent on open-graded.

The FHWA guidelines recommend using open-graded aggregate for the construction of

GRS-IBS because of the improved drainage ability and workability of this type of backfill compared to a well-graded aggregate.

2.1.1.2 Friction angle

The FHWA guidelines (Adams and Nicks 2018) recommend using a backfill material having a minimum friction angle of 38 degrees. This same experiment (Esmaili and Hatami 2015) also allowed the researchers to notice the variation in friction angle. The drier fill had a superior angle of friction than the wetter fill, however they were both under the threshold of 38 degrees recommended by the FHWA guidelines.

Another study performed by Ngo and Hatami (2016) used numerical modeling of existing GRS-IBS and altered some of the backfill and reinforcement characteristic values to evaluate the results. Three different values of friction angle were chosen for the backfill: the 38 degrees angle recommended by the FHWA guidelines, 34 and 44 degrees. The spacing of the reinforcement for all of them was of 8 inches. The results showed that "the lower backfill friction angle values consistently result[ed] in larger deformations" (Ngo and Hatami 2016). This observation could be done not only for the lateral displacement of the structure but also for the settlement values. Soil friction angle is an important parameter since it also governs the reinforcement-soil interaction angle.

2.1.2 Type of reinforcement

Another important component of a GRS structure is the type reinforcements used. Usually made of geosynthetic materials, those reinforcements are placed amongst the backfill material to form layers of reinforced soil. While geogrids can be used, geotextiles are more often used as reinforcements. From the FHWA guidelines (Adams and Nicks 2018), woven biaxial geotextiles

are preferred for their “ease of placement” and their “compatibility with the friction connection of the facing blocks used” (Adams and Nicks 2018).

2.1.2.1 Reinforcement spacing

Determining the impact of different backfill values on the performance of the GRS can be challenging because of the assumptions to make on a non-homogenous material, it is easier with reinforcements. The FHWA guidelines (2018) recommend using a layer spaced at a maximum of 0.3m (12 in) with an ultimate strength of at least 328.9 MN/m (4800 lb/ft). Changing the type of geotextile to one with a higher ultimate strength value is almost never done due to the increase of the cost per unit. Instead, the spacing between the layers can be adjusted to meet the stability requirement desired.

In their study, Ngo and Hatami (2016) compared the impact of two different spacings on the performances of the GRS-IBS using the numerical model discussed earlier. This experiment used spacings of 16 inches and 8 inches. As expected, the results for both settlement and horizontal displacement showed that the smaller spacing allowed for a more rigid structure overall. When coupled with a decreasing friction angle, the displacement increased even more.

Another study using numerical simulations evaluated the impact of optimal reinforcement density. Most of the time, the spacing of the main reinforcements stays the same on the total height of the structure. However, some benefits can be had by varying spacings, which allows for an optimal utilization of the reinforcements. In this study, the authors used two approaches to design the spacings. The “top-down” approach decreased the spacing from top to bottom, and the “bottom-up” approach increased the spacing from bottom to top. While observing the impact of varying reinforcements density, they also played with different geotextile tensile strengths and varying the footing setback relative to the front facing of the GRS. The length of the reinforcements

stayed the same for all scenarios. The backfill chosen to run those analyses had a friction angle of 34^{o} with no cohesion. The results of the simulations favored the top-down approach in terms of bearing capacity and stability of the structure when the structure had a surcharge applied to it. However, the bottom-up approaches had better benefits in stability when the structure was uncharged (Xie and Leschincky 2015).

2.1.2.2 Facing connection

The third-important element to consider is the facing connections. Indeed, the reinforcements need to be anchored somewhere to be sure that they do not slide when load are applied. Connection failure can also happen if the connection design was neglected by the engineer. Most of the time, segmental facing allows for frictional connection, meaning that the geotextile reinforcements are sandwiched between two facing elements.

In their study, Wu and Payeur (2014) did some stability analysis on segmental GRS walls. They did not use numerical models, field or lab experiments to complete this study. Instead, the authors started with the free body diagram of a typical GRS wall and developed generalized equations for driving and resisting forces at the reinforcement connection. The connection used would only be frictional. They then did the calculations using a backfill soil with a friction angle of 40 degrees with a wall height of 6 meters. They used a friction angle of 30 degrees for the geosynthetic-block interface. They also performed some tests using different values of soil friction and interfaces frictions. Their findings showed that the use of small reinforcement spacing, like those recommended by the FHWA guidelines at 0.3 m, allowed for more stability of the facing. On the other hand, large reinforcement spacing would give results more dependent on the friction angle. They also noted that some other ways to increase the connection strength was to increase the bulk weight of the facing blocks or use pins. However, they warn that “these measures tend to

attract more loads to the connection" and it might not "necessarily improve the facing stability" (Wu and Payeur 2014).

2.1.3 Type of facing

While the front facing technically has no purpose in the structural stability of the GRS-IBS structure, it can however play a role when it comes to the displacement and visual behavior of the abutment when loads are applied. A multitude of facing are used for basic GRS walls, but all of them are not suited to be used as the front facing of an abutment. The most commonly used type of facing in GRS-IBS is the segmental modular block wall. The block of choice is the concrete masonry unit (CMU) blocks, which should have nominal dimensions of 8 in × 8 in × 16 in with a minimum compressive strength of 4,000 psi (Adams and Nicks 2018). Theses blocks are widely used because of their simple and quick installation and the fact that they are lightweight, making their handling easy.

While the horizontal displacement of these blocks could become a problem, it is possible to take into account this displacement during the design phase and consider it when constructing the GRS-IBS on site. During the construction phase, the blocks are placed with an offset relative to their final position. When the wall gets further toward completion, they will come to their desired place on their own. The use of heavier facing blocks could be an option to reduce the horizontal displacement, but this could also bring its share of drawbacks.

The above studies show how the performance of the GRS-IBS technology can be altered when the main components characteristics are modified. However, to the best of the author's knowledge the important influence of the fill compaction effort on the stability and performance of the GRS abutment has not been addressed.

Chapter 3 – STUDY APPROACH

The study involved full-scale construction of GRS abutment models in an outdoor test station and ancillary testing of component materials in the laboratory, as described in detail in this section.

3.1 Test station

A significant part of the research study was carried out in the outdoor test station at Fears Structural Laboratory, as seen in **Figure 1**. The test station consists of an 8 ft × 8 ft × 20 ft reinforced concrete test box, a loading system and a shed that houses a data acquisition system, data loggers and uninterruptible power systems (UPS). The loading system is comprised of a steel frame, two hydraulic cylinders and corresponding 400-kip load cells, an electro-hydraulic loading pump, a loading beam and other ancillary components.

Figure 1 – Outdoor test station at Fears Structural Laboratory

3.2 Materials

3.2.1 Reinforcements

The Mirafi HP 570 polypropylene woven geotextile provided by TenCate Geosynthetics was used as reinforcement layers. This same geotextile was used for the previous iterations of GRS abutment models. This geotextile allows for an ultimate tensile strength of 4800 lb/ft for both the machine and cross-machine directions. It also has a strength of 1500 lb/ft strength at 2% strain in the cross-machine direction, according to the manufacturer Tencate.

3.2.2 Backfill

Two different types of aggregate were used for the construction of the GRS abutment models in this study (both supplied locally by Dolese Bros.): (1) 3/8" #2 Cover (**Figure 2a**), which is a nearly uniform, open-graded aggregate comparable in gradation to AASHTO 'Rock #89' used in field GRS-IBS projects; and (2) ODOT Type A (**Figure 2b**), which is a sub-one-inch, dense-graded aggregate. Details about the gradation of those two gravels will be discussed in **Section 4.1**.

(a) *(b)*

Figure 2 – Pile of aggregate at Fears Structural Laboratories: (a) 3/8" #2 Cover, (b) ODOT Type A

3.2.3 Equipment

3.2.3.1 Front loader and Jumping jack

A front loader tractor was used to load and move the aggregate from the piles to the test box. The jumping jack seen in **Figure 3** is a model Rammer MS780 from Chicago Pneumatic. It was used to compact the fill and realize the three compaction passes. The compaction process was carried out in a spiral pattern starting from the periphery toward the center of the GRS fill plan view.

Figure 3 – Jumping jack used for the compaction of GRS fill

3.2.3.1 Hydraulic cylinders and surcharge loading hydraulic pump

The surcharge load on the GRS abutment models was applied using two hydraulic cylinders that are mounted on the loading frame in the outdoor test station (**Figure 1**). A ¾ ft. × 8 ft. steel loading beam was used to transfer the applied load in the form of a line load at the top of the model

abutment to simulate loading from the beam seat of a bridge. The hydraulic cylinders were operated using a portable electro-hydraulic pump (**Figure 4**) that can apply the surcharge load in incremental steps. The hydraulic pump was connected to its own electrical outlet as it would otherwise generate electrical fluctuation when connected to the same electric strip as the other equipment in the shed.

Figure 4 – Portable electro-hydraulic pump

3.2.4 Instrumentation

3.2.4.1 Wire potentiometers

A total of 23 wire potentiometers (WP) were used to measure and record displacements and deformations of different parts of the abutment structure including its facing, settlements at the top, and reinforcement strains during construction and loading stages of the experiments. WPs were attached to target locations on selected reinforcement layers using steel wires, as shown in

Figure 5.

Figure 5 – Wire potentiometers being installed on one of the GRS abutment models

3.2.4.2 Earth pressure cells

Earth pressure cells (EPC) seen in **Figure 6** were placed under the central section of the facing column and inside the GRS backfill to record vertical pressures during construction and surcharge loading stages of the tests.

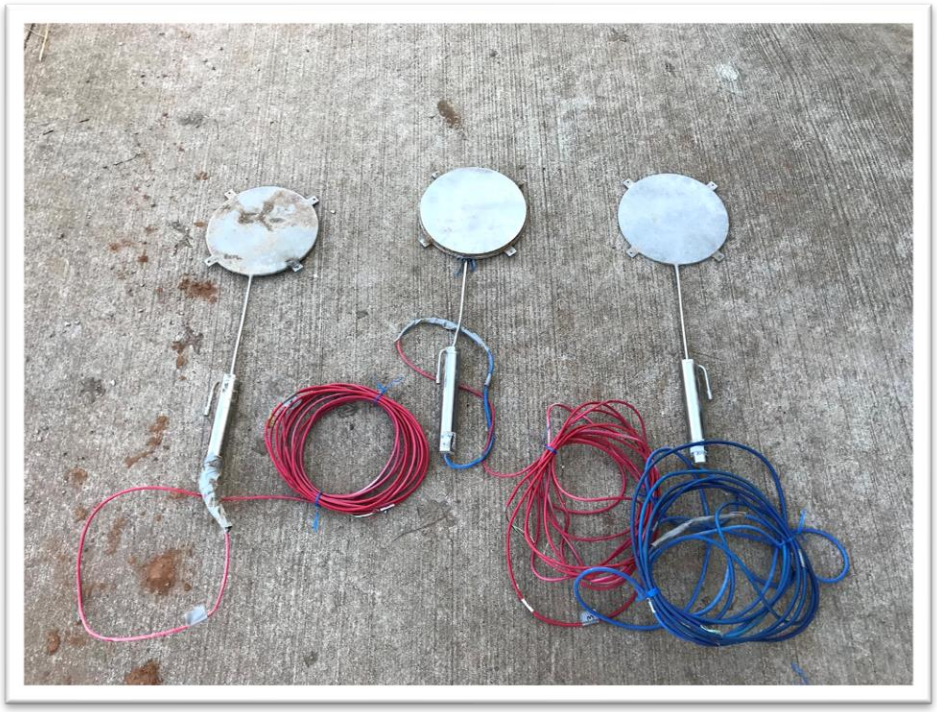

Figure 6 – Earth pressure cells

3.2.4.3 Load cells

Two 400-kip load cells, in blue in **Figure 7**, were used under the hydraulic cylinders of the loading assembly in the outdoor test station to measure applied loads on model GRS abutments during the performance load testing stage.

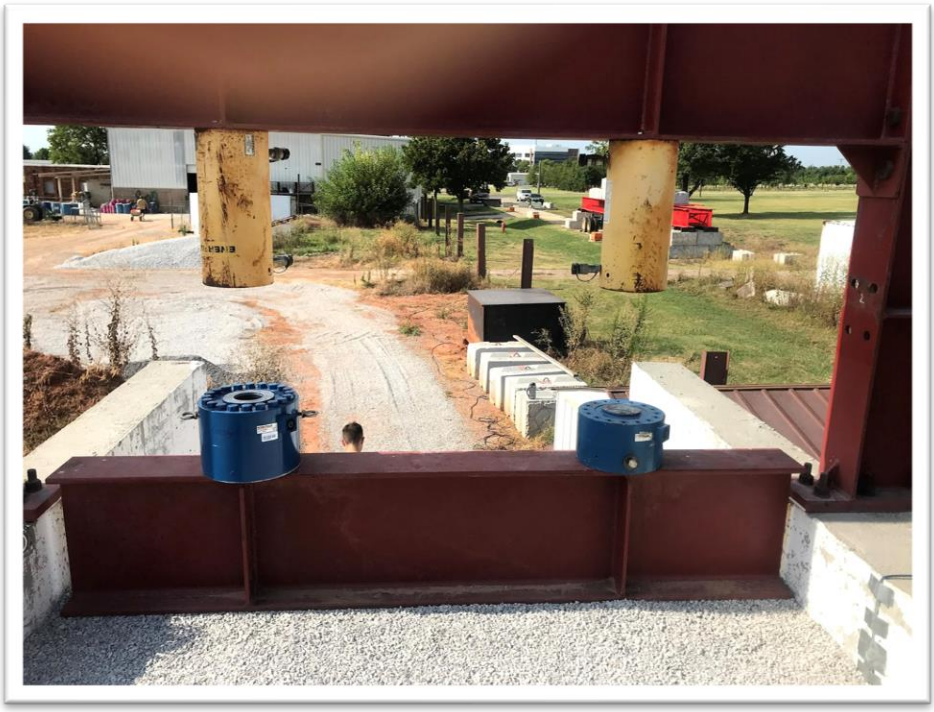

Figure 7 – Load cells (blue) on the loading beam

3.2.4.4 Data Acquisition System (DAS) and Dataloggers

Wire potentiometers (WP) and load cells (LC) were connected to an automated, 36-channel data acquisition and computer system to record and store the corresponding data for future analysis (**Figure 8**). Earth pressure cells (EPC) were themselves connected to a devoted data logger in a separated arrangement seen in **Figure 9**. The dataloggers gather and convert the data recorded by the load cells and transfer them to a computer. Two different dataloggers, models 8002-16 and 8021-1X, were used simultaneously when the EPCs were under usage. The DAS, dataloggers and computers were all connected to devoted UPS units inside the shed in the outdoor test station for power surge and outage protection.

Figure 8 – WP and LC computer setup

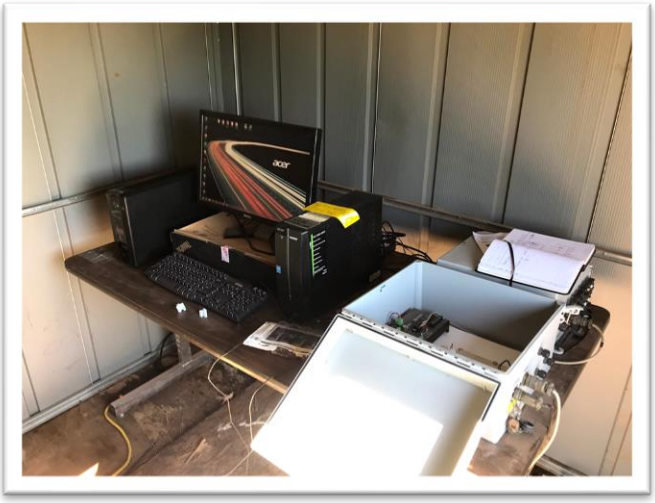

Figure 9 – EPC Datalogger and computer setup

Chapter 4 – ANCILLARY TESTING

In this part of the thesis is detailed the several ancillary tests that had to be carried out to meet the project ends. For each test, a brief introduction and explanation is given before going through the results and analysis.

4.1 Sieve analysis of #2 Cover and ODOT Type A aggregates

Before doing any tests on fill aggregates at the Fears Laboratory, a series of sieve analyses were carried out on samples in conformance with the ASTM C136 test protocol. The same aggregates were reused for the first three GRS models. Because of repeated compaction and testing on the materials, a noticeable shift in their gradation could have appeared. For this reason, the gradation was determined and monitored to decide if new deliveries of aggregate materials were necessary.

According to the ASTM C136, a minimum of 1 kg is necessary to carry out sieve analysis on #2 Cover samples because of the maximum grain size of the aggregate, which is 3/8 in. For the ODOT Type A, with a maximum grain size of 1 in, at least 10 kg of samples need to be sieved. To provide the most accurate representation of the piles possible, the samples of gravel were taken from each sides of the piles. The deposit piles for both types of aggregate were roughly 30 feet in length and width with a height of 7 feet.

Before sieving, the samples were oven dried at a temperature of 110 ±10C°. The sieving was performed using the sieves and shaker equipment available at the soils and geosynthetics laboratories. The sieves used for the two aggregates are shown in **Table 1**. Those were selected to match those in the supplier's sieve analysis report and in conformance with the ASTM C136 test protocol.

Reduction of the sieve analysis data consists of measuring the percentage of soil (by

weight) that passes through each sieve size for each aggregate sample. The results for different samples were averaged to determine the gradation of each aggregate. Those results were then subsequently compared with those recommended in FHWA guidelines for open-graded (AASHTO No. 89) and well-graded aggregates (VDOT 21-A), as shown in **Table 1**.

Table 1 – FHWA recommendations vs. actual aggregates used in the study

Sieve Size	FHWA Recommendation AASHTO #89 (Open graded) weight % passing	FHWA Recommendation VDOT 21-A (Dense graded) weight % passing	Actual Aggregate Used 3/8" #2 Cover (Open graded) weight % passing	Actual Aggregate Used ODOT Type A (Dense graded) weight % passing
2"	--	100	--	100
1"	--	94-100	--	98
½"	100	--	98	73
3/8"	90-100	63-72	80	--
No. 4	20-55	--	6	41
No. 8	0-15	--	1	--
No. 10	--	32-41	--	23
No. 16	0-10	--	1	--
No. 40	--	14-24	--	8
No. 50	0-5	--	1	--
No. 200	--	6-12	0	1

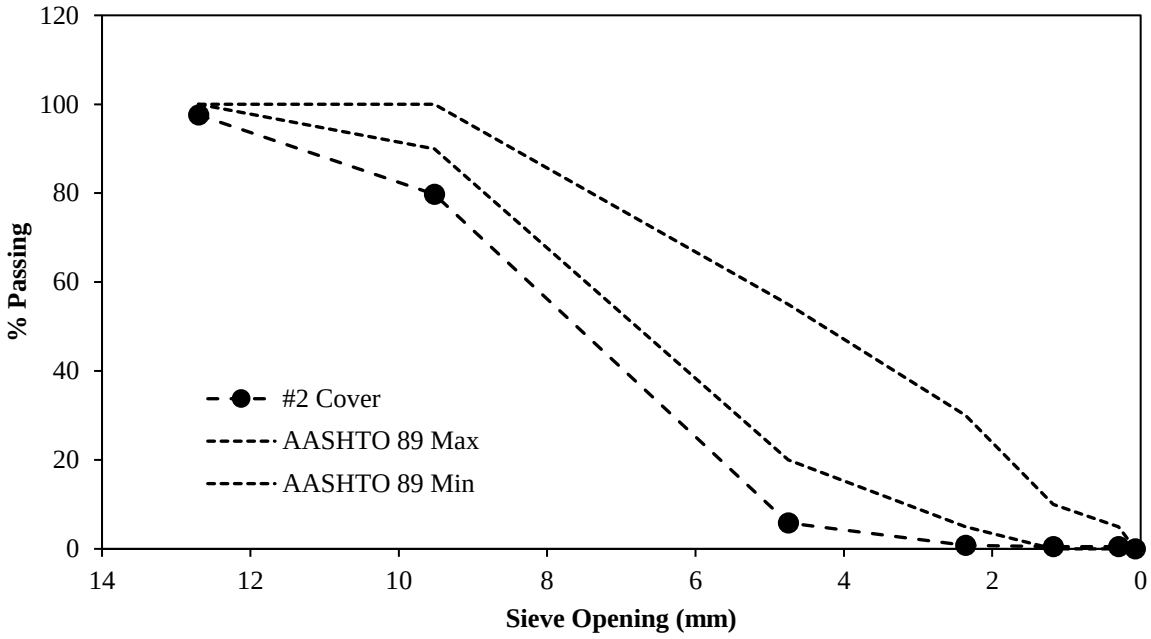

(a)

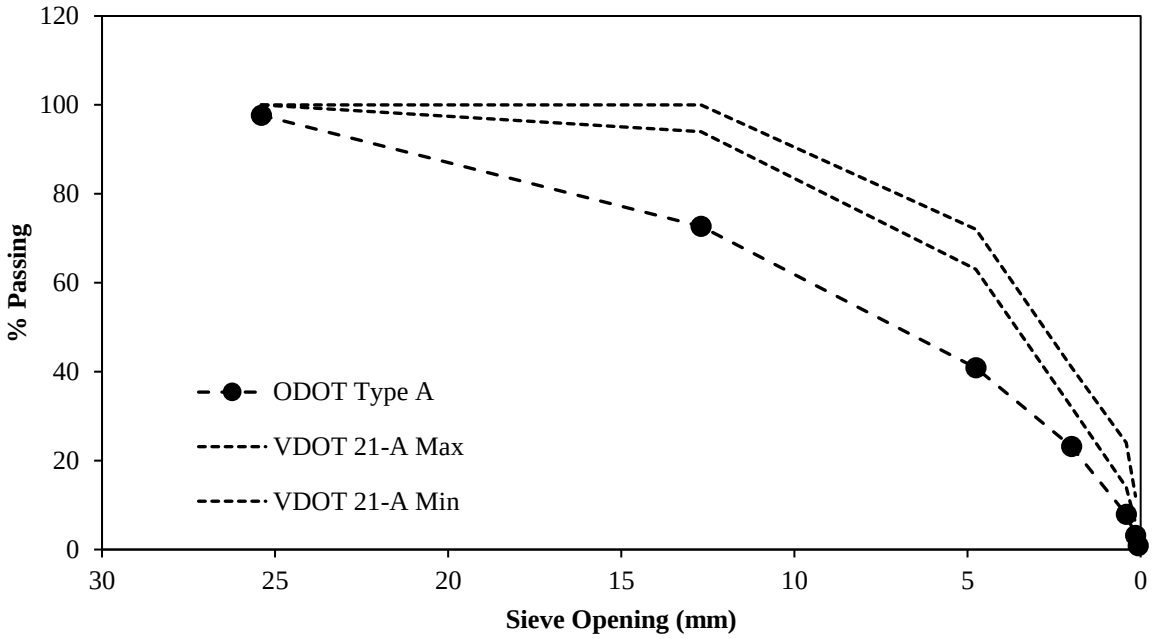

(b)

Figure 10 – Gradation curves of the aggregates: (a) #2 Cover, (b) ODOT Type A

As seen in **Table 1** and **Figure 10**, the #2 Cover is indeed a uniformly and open graded gravel with a low fine percentage to allow good drainage. On the other hand, the ODOT Type A has a wide range of particles sizes, especially small ones, rendering it densely graded and less appropriate for drainage purposes.

4.2 Unit weight determinations

A main objective of this study was to examine the influence that compaction effort and the resulting fill unit weight can have on the load-bearing capacity and performance of GRS abutments. Therefore, a series of tests were carried out using both standard-size samples of fill aggregates in the laboratory and large-scale test beds to determine the relationship between the compaction effort and the resulting unit weight of the fill aggregates, as described in this section.

4.2.1 Relative unit weights as per ASTM D4253

A series of tests were realized to determine the range of unit weight values for the aggregates in the laboratory, mainly in conformance with the ASTM D4253 test protocol. The equipment for these tests is pictured in **Figure 11**. The table used for this test was however not the standard used by the ASTM as it was too small and light. To try and counteract this fact, the samples were vibrated for at least 16 minutes, instead of only 8 minutes at 60 Hz.

The mold is filled with gravel and the initial height is taken to determine the loose unit weight of the gravel. Before the vibration period begins, a weight of 200 pounds is laid on top of the gravel. To prevent any injuries, a small hydraulic crane is used to lift and move the weight. Once the vibration is done, the height is taken again and the final, theorical maximum density can be determined.

Figure 11 – Assembled relative density test apparatus

The results obtained after running the test on both #2 Cover and ODOT Type A are shown in **Tables 2 & 3** and **Figure 12**.

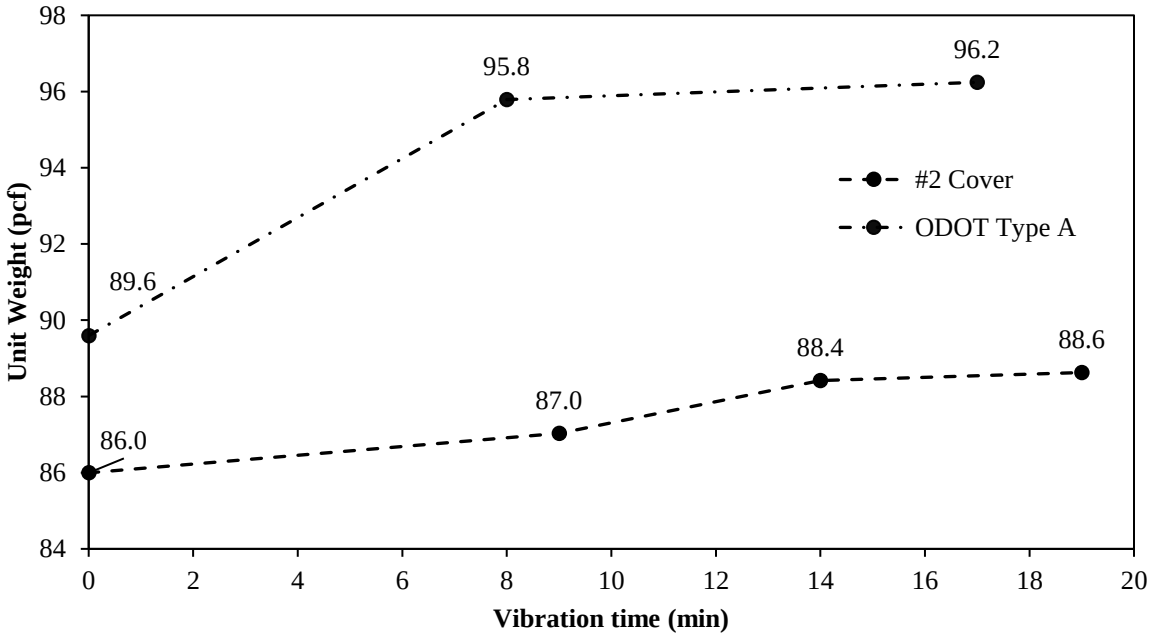

Figure 12 – Unit weight of each aggregate as a function of vibration time

Table 2 – Unit weight variation of the #2 Cover aggregate

Phase	**Sample height**		**Unit weight**
Initial height reading	H_i	9.092 in	**86.0 pcf**
9 min @ 90% Power	H_{f1}	8.984 in	87.0 pcf
14 min @ 90% Power	H_{f2}	8.843 in	88.4 pcf
19 min @ 100% Power + Hammering	H_{f3}	8.822 in	**88.6 pcf**

Table 3 – Unit weight variation of the ODOT Type A aggregate

Phase	**Sample height**		**Unit weight**
Initial height reading	H_i	9.092 in	**89.6 pcf**
8 min @ 100% Power	H_{f1}	8.504 in	95.8 pcf
17 min @ 100% Power	H_{f2}	8.464 in	**96.2 pcf**

Results compiled in **Figure 12** and **Tables 2 & 3** show that the ODOT Type A is indeed denser than the #2 Cover, even in its loose state. The ODOT Type A is also much more

compressible than the #2 Cover as seen by the difference between their loose state and maximum density unit weight values.

It needs to be noted that the data extracted from these experiments could have been influenced by the vibrating table used. The table weight being too low could have caused issues such as the energy transferred to the gravel or the amplitude of the vibration being too small.

4.2.2 Test bed for large-scale compaction and unit weight experiments

The purpose of the test bed was to determine the compaction effort needed to compact the #2 Cover to a target unit weight using the same compactor equipment that was used to build the GRS model abutments. The inside dimensions of the test bed were in the form of a 4 ft-side cube, as shown in **Figure 13.** These dimensions were deemed to be large enough to not have to deal with the scale effect. The test bed was confined with the concrete walls of the outdoor test box in a corner, and four large (i.e. 2' × 2' × 4') concrete blocks which are also intended for use as facing of GRS abutment models in a subsequent stage of the study.

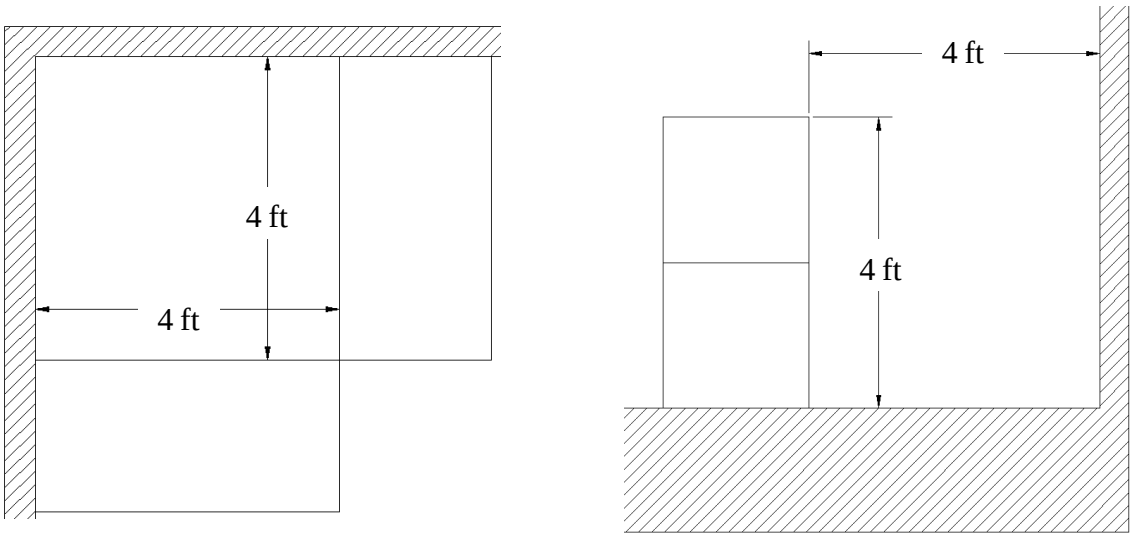

(a) *(b)*

Figure 13 – Schematics of the test bed: (a) Plan view, (b) Cross sectional view

The procedure works as followed. The test bed was filled with aggregate in 8-inch lifts and was compacted with the jumping jack. The weight of the aggregate necessary to complete each lift was measured and documented. Once the test bed was completely full, its total volume and total weight of compacted aggregate were used to determine the as-placed weight of the aggregate representing the condition in subsequent full-scale GRS abutment models. This procedure was repeated twice for each compaction mode: one pass and three passes. This was done for comparison purposes and to ensure that the values obtained were coherent. No power settings are available on the jumping jack, but the compaction was carried out consistently with the choke fully open and the throttle set to its maximum.

The results of the different test bed experiments are shown in **Table 4**.

Table 4 – #2 Cover compaction test bed results

	One pass		**Three passes**	
Test 1	102.2 pcf	**101.6 pcf**	104.9 pcf	**105.1 pcf**
Test 2	101.0 pcf		105.2 pcf	

Given these results, it appears that the #2 Cover gravel has an average unit weight of **101.6 pcf** when compacted once and **105.1 pcf** when compacted three times. The values obtained while doing the experiment twice for each compaction effort are close to each other. This means that the unit weight obtained can be considered plausible. If those experiments were run again, it would be expected to find values in the range of what was obtained here.

However, when those values are compared to those obtained when performing the relative density tests, a noticeable difference in values can be seen. The maximum density for the #2 Cover that was found with the relative density test is 88.6 pcf. But as said in the previous section, these low values could have been the results of the test apparatus not being completely conform to the

ASTM standard. Other errors could have come from several factors related to the test bed experiment itself. The weight of the gravel could have been artificially increased because of the presence of moisture. The compaction of the corners of the test bed was hard to do mainly because of the difficulty to handle the jumping jack in a tight space such as this one. The interior surface and walls of the test bed might also not be completely even, meaning that the volume calculated does not precisely reflect the actual volume. Also, the jumping jack is applying a compaction effort intensity that cannot be replicated by the relative density test apparatus.

4.3 Direct Shear Tests

A series of Direct Shear Tests (DST) were carried out to determine the friction angle, ϕ of the GRS fill aggregates. The tests were carried out at different unit weights, including those determined from the test bed experiments described in the previous section. The DST were carried out in conformance with the ASTM D3080 test protocol.

Figure 14 shows the large-cell (1 ft × 1 ft plan area) DST machine, available in one of the Geosynthetics laboratories at OU, was used to run the tests. This machine allows for nearly 2/3 of a cubic foot of aggregate to be tested at once. In the tests relevant to this study, the aggregate was placed in the test cell in its loose state, as is it in no way manually possible to replicate the effort applied by the compactor on the gravel. This also means that the values deducted from these tests are the lower boundary values for the materials, and that these could very well be higher when the gravel is compacted. A target overburden pressure is applied, the specimen is then sheared along a horizontal plane at its mid-height at a fixed shear (displacement) rate. Two LVDTs are used to measure and record vertical and horizontal displacements of the specimen during the test. Each test at a set gap size was run at least three times under different overburden pressure values to determine the corresponding friction angle for the tested aggregate material.

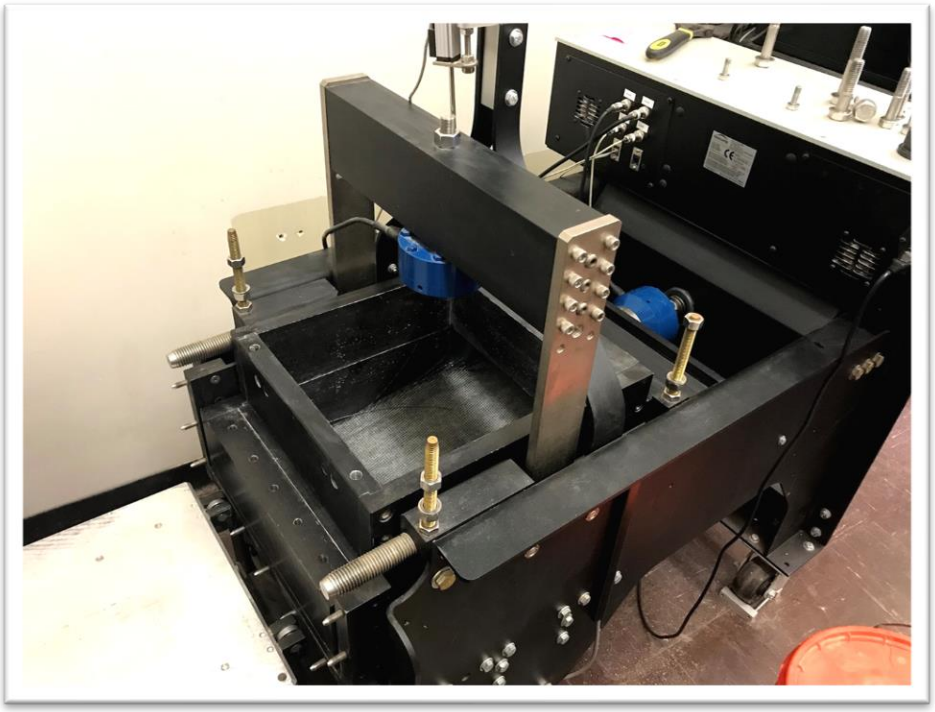

Figure 14 – Direct Shear Test machine

For all the tests, the shear rate was of 0.5 in/min for a total horizontal displacement of 2 inches, allowing a short test duration and maximize the number of tests realizable in one session. A superior horizontal displacement would not be possible because of the physical limitation of the apparatus.

Tables 5 and 6, and **Figures 15 and 16** show the results of the DSTs ran on both #2 Cover and ODOT Type A gravels.

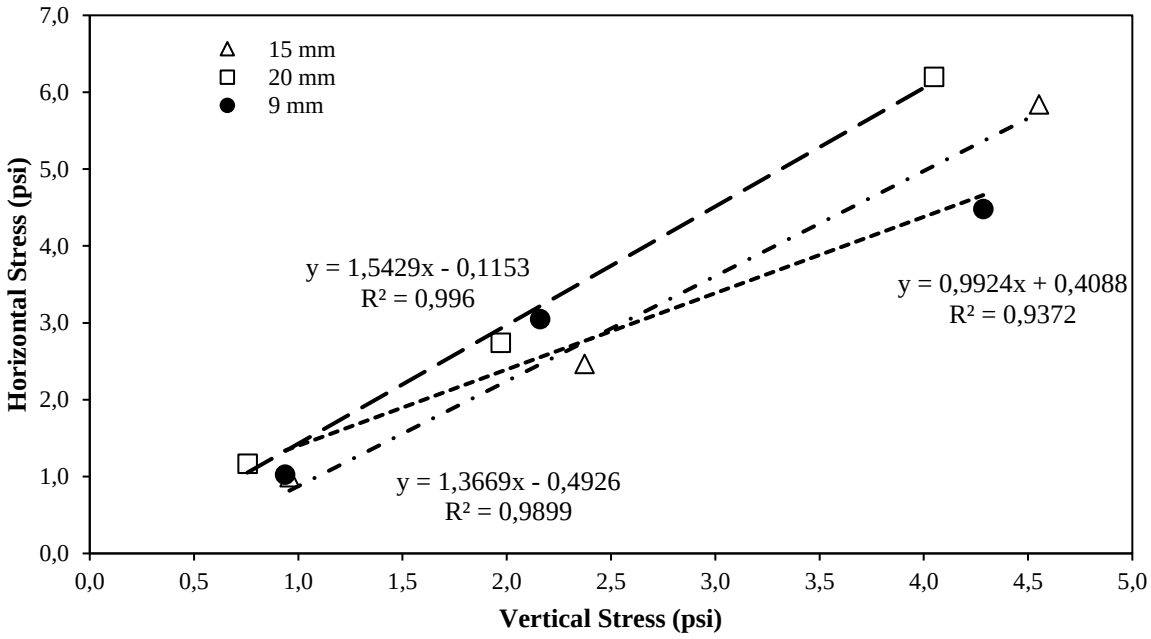

Figure 15 – #2 Cover - Peak Friction Angle – Loose State

Table 5 – #2 Cover - Peak Friction Angle – Loose State

Peak friction angle - Loose - 9 mm gap			
	sigma_v (psi)	tau_max (psi)	Peak Angle (°)
Loose - 5 kPa - 9 mm	0.94	1.02	
Loose - 15 kPa - 9 mm	2.16	3.05	44.8
Loose - 30 kPa - 9 mm	4.29	4.48	
Peak friction angle - Loose - 15 mm gap			
	sigma_v (psi)	tau_max (psi)	Peak Angle (°)
Loose - 5 kPa - 15 mm	0.96	0.99	
Loose - 15 kPa - 15 mm	2.37	2.46	53.8
Loose - 30 kPa - 15 mm	4.55	5.84	
Peak friction angle - Loose - 20 mm gap			
	sigma_v (psi)	tau_max (psi)	Peak Angle (°)
Loose - 5 kPa - 20 mm	0.76	1.17	
Loose - 15 kPa - 20 mm	1.97	2.74	57.1
Loose - 30 kPa - 20 mm	4.05	6.20	

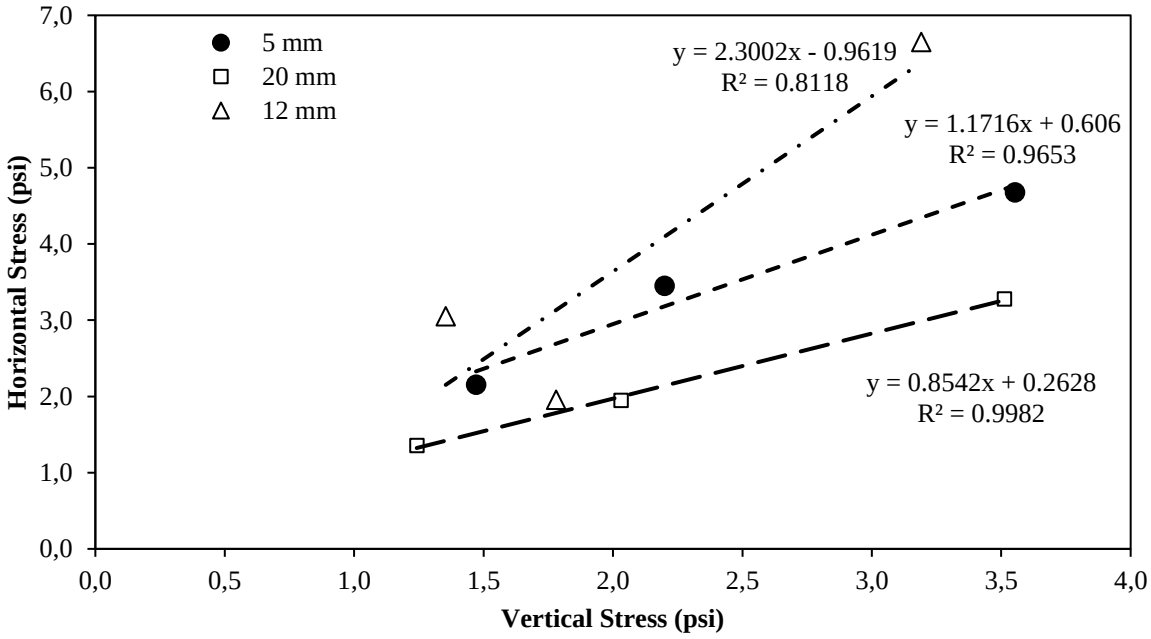

Figure 16 – ODOT Type A - Peak Friction Angle - Loose State

Table 6 – ODOT Type A - Peak Friction Angle - Loose State

Peak friction angle - Loose - 5 mm gap			
	sigma_v (psi)	tau_max (psi)	Peak Angle (°)
Loose - 10 kPa - 5 mm	1.47	2.16	
Loose - 15 kPa - 5 mm	2.20	3.45	49.52
Loose - 25 kPa - 5 mm	3.55	4.68	
Peak friction angle - Loose - 12 mm gap			
	sigma_v (psi)	tau_max (psi)	Peak Angle (°)
Loose - 10 kPa - 12 mm	1.35	3.05	
Loose - 15 kPa - 12 mm	1.78	1.96	66.50
Loose - 25 kPa - 12 mm	3.19	6.65	
Peak friction angle - Loose - 20 mm gap			
	sigma_v (psi)	tau_max (psi)	Peak Angle (°)
Loose - 10 kPa - 20 mm	1.24	1.35	
Loose - 15 kPa - 20 mm	2.03	1.95	40.51
Loose - 25 kPa - 20 mm	3.51	3.28	

While doing this experiment, the influence of the gap size was also monitored. The gap size refers to how spaced out the top and bottom boxes are during the shearing phase of the test. The ASTM D3080 considers that the gap should be approximately equal to the maximum grain particle size of the material being tested. For the #2 Cover the ideal gap would be 9 mm, while it would be 12 mm for the ODOT Type A. The other gap sizes were selected arbitrary, just as a mean to see their influence on the friction angle obtained but also to have control values. As seen from the results above, some of the friction angles obtained seem to be plainly wrong as they manage to attain values that should not be possible with these types of materials. Considering only the values that are plausible, it appears that both the #2 Cover and the ODOT Type A have a peak shear angle of 45°.

Since the ODOT Type A can be compacted to denser states than the #2 Cover, it was expected that it would have a higher peak friction angle. However, it needs to be noted that during the tests done on the ODOT Type A, the specimen would not be completely sheared off. This was deduced by the fact that the horizontal displacement versus horizontal stress curves had not plateaued and trend downward by the time 2 inches of horizontal displacement has been reached. To completely shear the material, more than 2 inches of displacement would have been needed, but as said earlier the physical limitations of the machine do not allow that. This hardware limitation on the horizontal displacement is also why the residual friction angles of the gravel was not determined as the specimen do not have the space to go into post-shearing phase.

With these ancillary tests taken care of, the rest of this thesis will now fully focus on its main topic: the construction and testing of the new GRS abutment models.

Chapter 5 – CONSTRUCTION AND LOAD TESTING OF GRS ABUTMENT MODELS

The main part of this research project involved the construction and performance testing of three (3) GRS abutment models in the outdoor test station at the Fears Structural Laboratory to attain the objectives described in **Section 1.3**. The procedure is described in more detail in this section.

5.1 Descriptions of the GRS abutment models

Figure 17 shows schematic cross-sections of the three GRS abutment models that were constructed and tested in this study. These models are numbered #4 through #6 as they are part of a long-term research program on GRS bridge abutments in which three earlier full-scale models have already been built and tested before this study. Therefore, the numbers for models from the previous study that are comparable to those in this study are also indicated in the figures for comparison purposes.

The instrumentation plan was based on the anticipation that a potential global slip plane under load levels greater than the service load of 4 ksf would initiate from the heel of the loading beam and propagate downward toward the toe of the GRS mass.

Models #4 and #5 are the same as Model #1 (from previous study) except that three passes of compaction (as opposed to one pass only in the previous study) were applied on each 8 inch-lift during its construction. This allows for a direct comparison between the models to quantify the influence that compaction effort would have on load-bearing capacity and performance of GRS abutments at full scale. Both models include 90-inch-long reinforcement layers at 8-inch spacing with an additional block of shorter reinforcement at 4-inch spacing immediately underneath the loading beam as per the FHWA guidelines (Adams et al. 2012, 2018). All three models in this

study were built using CMU blocks as for their facing. Models #4 and #6 are similarly instrumented with wire potentiometers, earth pressure cells and load cells to measure their construction and loading performances. However, Model #5, which is nominally identical to Model #4, was built without internal instrumentation in order to isolate the construction time that is specifically devoted to the model construction from any interference due to instrumentation-related activity. This model provides additional performance data relative to its load bearing and deformation performance to compare against those on Models #1 and #4. Moreover, it additionally provides valuable data on the actual construction time anticipated for GRS abutments in the field.

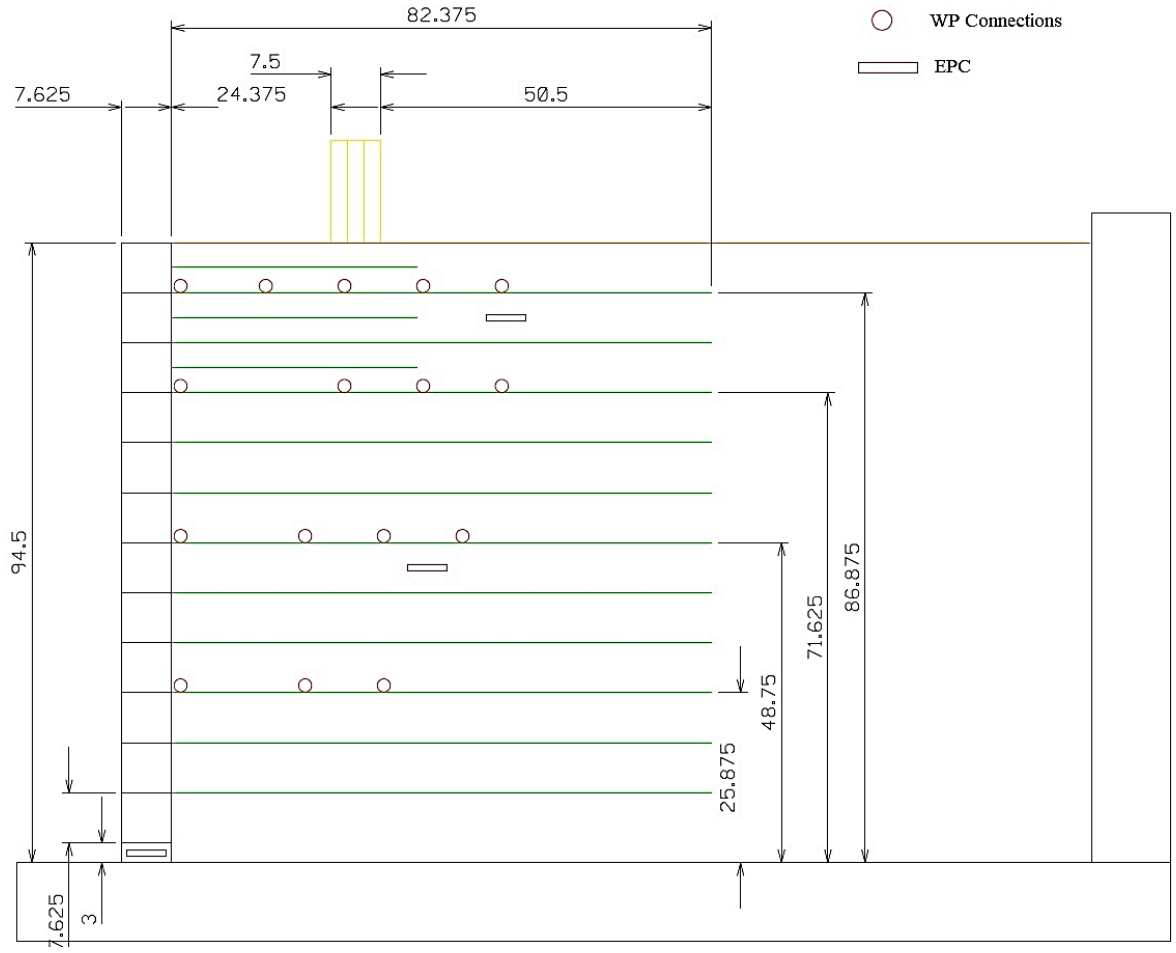

Figure 17 – Schematic cross section and instrumentation plan for GRS Abutment Models #4 - #6. Model #5 will not include internal instrumentation. Dimensions are in inches (Adopted from Doger 2020).

Model #6 was built with a dense-graded aggregate, which was also compacted using three (3) passes of the compactor equipment. The aggregate used for the backfill was the ODOT Type A with a gradation comparable to what is shown in **Table 1 (Section 4.1)**.

5.2 Construction

5.2.1 Preliminary preparations

Geotextile sheets were cut to the right dimensions for all 11 layers of reinforcement. Each reinforcement layer includes one wide geotextile sheet and two narrow ones, all of them having the same length of 90 inches. For the top three layers mid-layer reinforcements were placed, having half the length of the primary reinforcements.

The deformation of four of those geotextile layers were monitored using wire potentiometers. Because of that, wires need to be attached on the specific geotextiles beforehand, as seen on **Figure 18**. The attachments onto the geotextile were done using bolts, nuts and washers.

Figure 18 – Instrumented geotextile sheet before being put into a GRS model

Additionally, the instrumentation used to monitor the behavior of the structure had to be tested and calibrated. The WPs need to be able to give accurate values of length while the EPCs need to give the right pressure value.

5.2.2 Construction of the GRS

The first step in the construction was to place the three base EPCs underneath the first layer of CMU facing blocks (**Figure 19**). The EPCs were placed on a sand bed, leveled and covered with sand again so that the pressure they are measuring is well dispersed. The sand also protects the EPCs themselves and their wires from the sharp edges of the aggregate. For each layer, the construction process was always be the same. The CMUs were placed, providing an elevation reference as to where the backfill needs to go up to. The necessary gravel to completely fill up the layer was placed using the front loader tractor.

Figure 19 – Base EPCs underneath the facing column

The gravel was then evenly spread and leveled before the jumping jack compactor was brought in to do the three passes of compaction. Near the facing, the compaction was done using a hand tamp to prevent too much movement outward from the facing blocks. The position of the facing was also monitored manually before and after each compaction cycle to see its impact on the facing. Finally, the geotextile reinforcements were placed and sandwiched between two layers of CMU facing blocks and the cycle begins again.

It needs to be noted that because of the ODOT Type A aggregate properties, this material was harder to work with. After a rainy day for instance, the gravel would just dry up and harden enough to form clumps that needed to be broken up. This aggregate was also rather difficult to compact since it would just push the CMU blocks away when trying to compact right behind the facing, even with hand compaction. Compacting with the jumping jack would also cause the

aggregate to settle for about 1 inch compared to its loose state. All those issues were not present when using the #2 Cover aggregate.

The reinforcement layer at the elevations 27, 51, 75 and 91 inches were equipped with instrumentation for the wire potentiometers. Only the center section of the reinforcement was instrumented. The steel wires ran through the back wall of the test box and were connected to the wire potentiometers attached there (**Figure 20**). Sand was placed on the wires themselves to prevent the gravel from causing any harm to them (**Figure 21**).

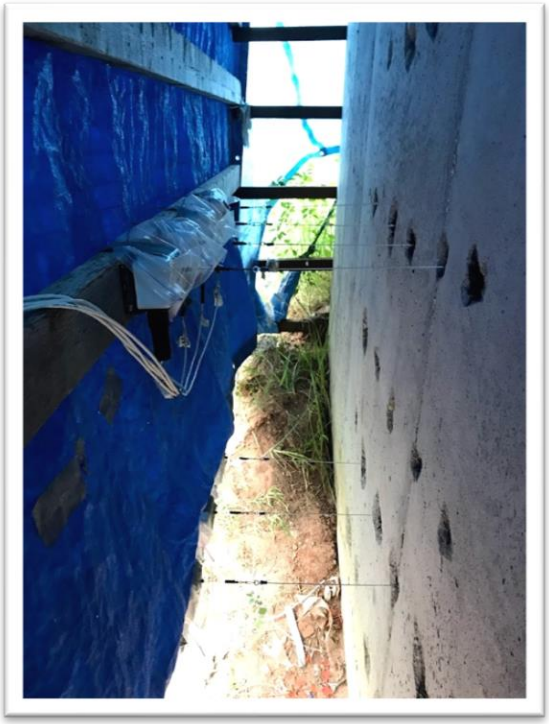

Figure 20 – Wire potentiometers at the back

Figure 21 – Wires protected with sand

At the elevations 47 and 87 inches, an EPC was placed in the bulk of the GRS to measure the pressure inside of the structure as seen in **Figure 22**. As for the base EPCs, there were laid on a bed of sand, leveled and covered with sand for protection. For the top three layers, the facing was reinforced using rebars and concrete poured through the hollow CMUs (**Figure 23**).

The compaction of the last layer was done as close as possible to the start of the performance test as the backfill would just swell again since there was no confining pressure on it.

Figure 22 – EPC placed in GRS fill

Figure 23 – Top three courses of CMU infilled with rebars and concrete

5.3 Performance tests

After each model GRS abutment was fully constructed, it was subjected to a strip footing surcharge load behind its facing, simulating bridge load, to examine its load-bearing capacity and resulting deformations.

Using a combination of hydraulic cylinders hooked up to a hydraulic pump, the load was applied in increments of 10-20 kips until reaching a total surcharge of 200-250 kips or a settlement greater than 2 inches. The horizontal displacement of the structure was also closely observed throughout the tests. To monitor the load applied by the cylinders, load cells were placed between the cylinders and the loading beam. The whole setup was secured using straps and chains attached to the different components, preventing them from getting ejected in case of a potential failure (**Figure 24**).

Figure 24 – Hydraulic cylinders, load cells and loading beam

At the front of the GRS, wire pots measuring the displacement of the facing during the test were set up. Additionally to those, wire pots measuring the settlement of the beam were placed on top of the structure (**Figure 25**).

During the tests, data from all sensors were collected for later analysis. Primary output of interest includes load-settlement performance of each abutment, which were compared across all models and with those of the models tested in a recent study (Doger et al. 2019) in addition to facing deformations, reinforcement strains and earth pressures in selected locations in the GRS fill. Discussion on the output results are thoroughly discussed about in **Chapter 6**.

Figure 25 – Front of the test set up with the wire potentiometers Dismantlement

5.4 Excavation and survey

After each test was completed and the data collected, the model was completely dismantled to make room for the next one. The excavation was done layer by layer carefully as to not damage the instrumentation but also to perform a survey of the structure and assess the impact of the loading test on the layers, as seen in **Figure 26**.

GRS#6 also had its backfill density monitored, as the dense graded fill allowed for the use of a sand cone apparatus. More details can be found in **Section 6.6**.

Figure 26 – Top GRS layer being excavated

Chapter 6 – RESULTS

In this section of the thesis is presented, analyzed and discussed the results that were gathered from the construction, testing and dismantling of the GRS abutment models. **Table 7** summarizes different outcomes corresponding to the comparison of selected model performances to further help with the interpretation of the test results provided in this section. Since the focus of this study is on GRS models #4 through #6, the comparisons that are made here are only those that are relevant to this study. Any comparisons between GRS models #1 through #3 will not be done here.

Table 7 – Outcomes from the comparison of different abutment models in relation with this study

Model #	Outcome
1,4,5	Performance verification of control model with most commonly used materials
4,6	Influence of backfill type
1,4	Influence of compaction effort
4,5,6	Influence of the crew experience on construction speed

6.1 Load Settlement performance

Figure 27 shows load-settlement response of the beam representing the bridge abutment for all CMU facing GRS models tested in this project, which were subjected to a minimum of 200-kip surcharge load.

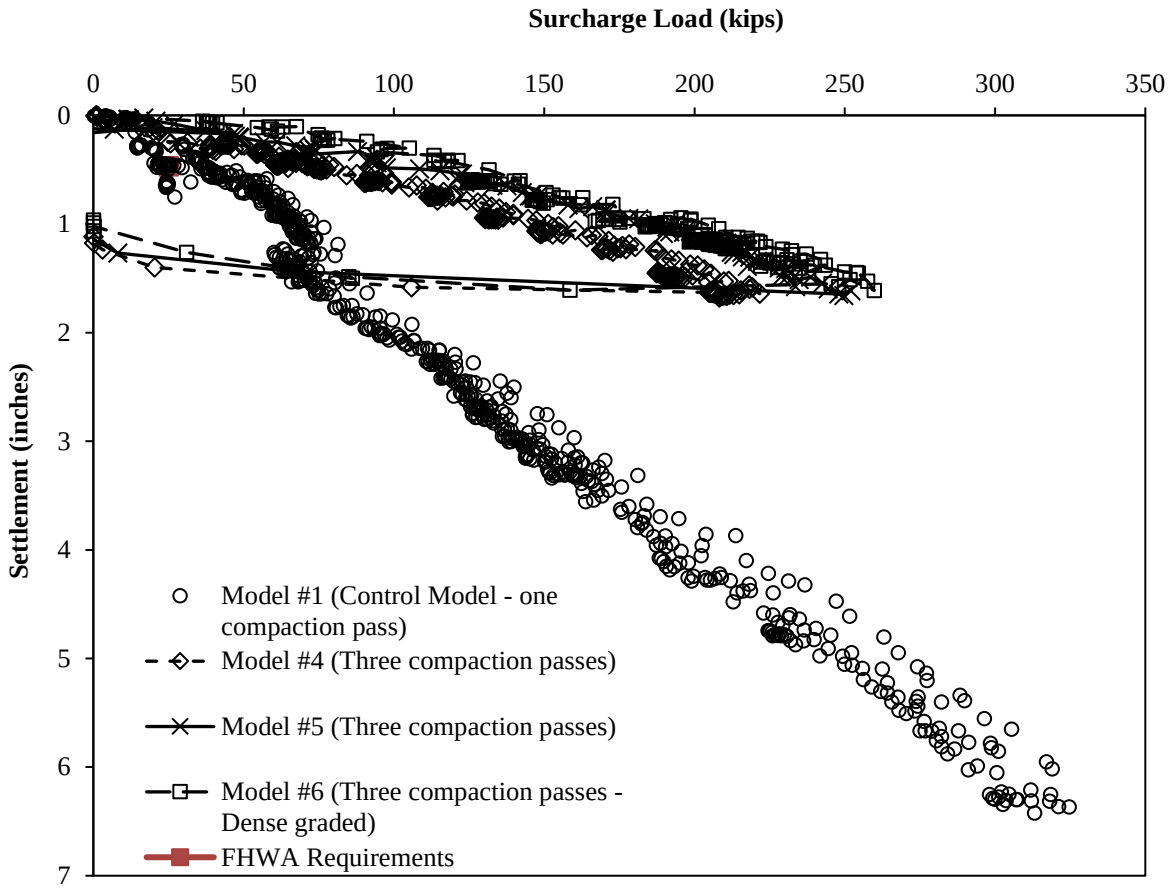

Figure 27 – *Load-settlement responses of GRS Abutment Models #1 and #4 through #6*

Comparison of the results in **Figure 27** shows how the backfill compaction effort could affect (even for the more uniform open-graded fills) the performance of GRS abutments. For instance, the measured amount of settlement in Model #1 (with reduced compaction effort) at 200 kips of surcharge load is approximately 3.2 inches. In comparison, the corresponding magnitudes of settlement (at 200 kips) in Models #4 - #6 are 1.4, 1.1 and 1.0 inches, respectively. These are equal to, or only slightly greater than, the limiting value of 1 inch (Adams *et al.* 2012, 2018) for the service load of 25 kips for the model abutments in this study.

Models #4 - #6 that were built with recommended compaction effort (i.e. three passes of compactor per lift) all show significantly smaller settlements relative to Model #1. They also all

allow for significantly larger surcharge loads that what the FHWA recommended value is (i.e. 20kips for 0.47 inches).

Models #4 and #6 were built as a mean to gauge the influence of backfill type on the performance of the structure. Results in **Figure 27** show that open graded and dense graded fill virtually gave the same performance. While the dense graded fill was predicted to bring better performance, these underwhelming results could be the cause of several factors. First factor is the rather poor workability of the gravel that made it difficult to evenly spread out the gravel. Another influence is the difficulty to compact the material that was right behind the facing blocks without warping the facing. With a better approach and specialized tools, it is safe to say that the dense graded fill would have provided better performance than those.

With a required service load of 4 ksf determined by the FHWA (Adams et al. 2012a, b, 2018), Models #4 - #6 have Factors of Safety (FoS) of 11.0, 12.6 and 13.0 respectively. These FoS were calculated using the highest surcharge load that was achieved during the performance tests.

6.2 Excavation Survey

(a) (b)

Figure 28 – Excavation of the 12th layer: (a) Model #5, (b) Model #6

Figure 28 shows the different behavior of the two gravels when the linear load representing the bridge deck is applied to them. Both figures show the model with the top layer removed and uncovering the geotextile reinforcement of the 11th layer. On Model #5 using the open graded fill, the settlement is clearly visible and focused right under where the loading was applied. This focused depression is still visible two layers down.

On the other hand, Model #6 using dense graded fill does not show this focused settlement area. As seen on **Figure 28b**, the settlement area is more spread out and that same pattern is found on the two directly underlying layers.

This difference in behavior could come from the fact that the open graded gravel gets crushed and create smaller particles taking less volume. The dense graded gravel just rearrange itself as it already has a high proportion of smaller particles.

6.3 Facing deformation

6.3.1 During the construction

While constructing the abutment Model #4, the displacement of the facing during construction was manually monitored to survey the effect of the compaction effort on the unwanted displacement of the CMU blocks at each level. The contour map in **Figure 29** shows the cumulative displacement of the center section of the facing due to compaction at the end of the construction phase. Six measurements were taken on each row.

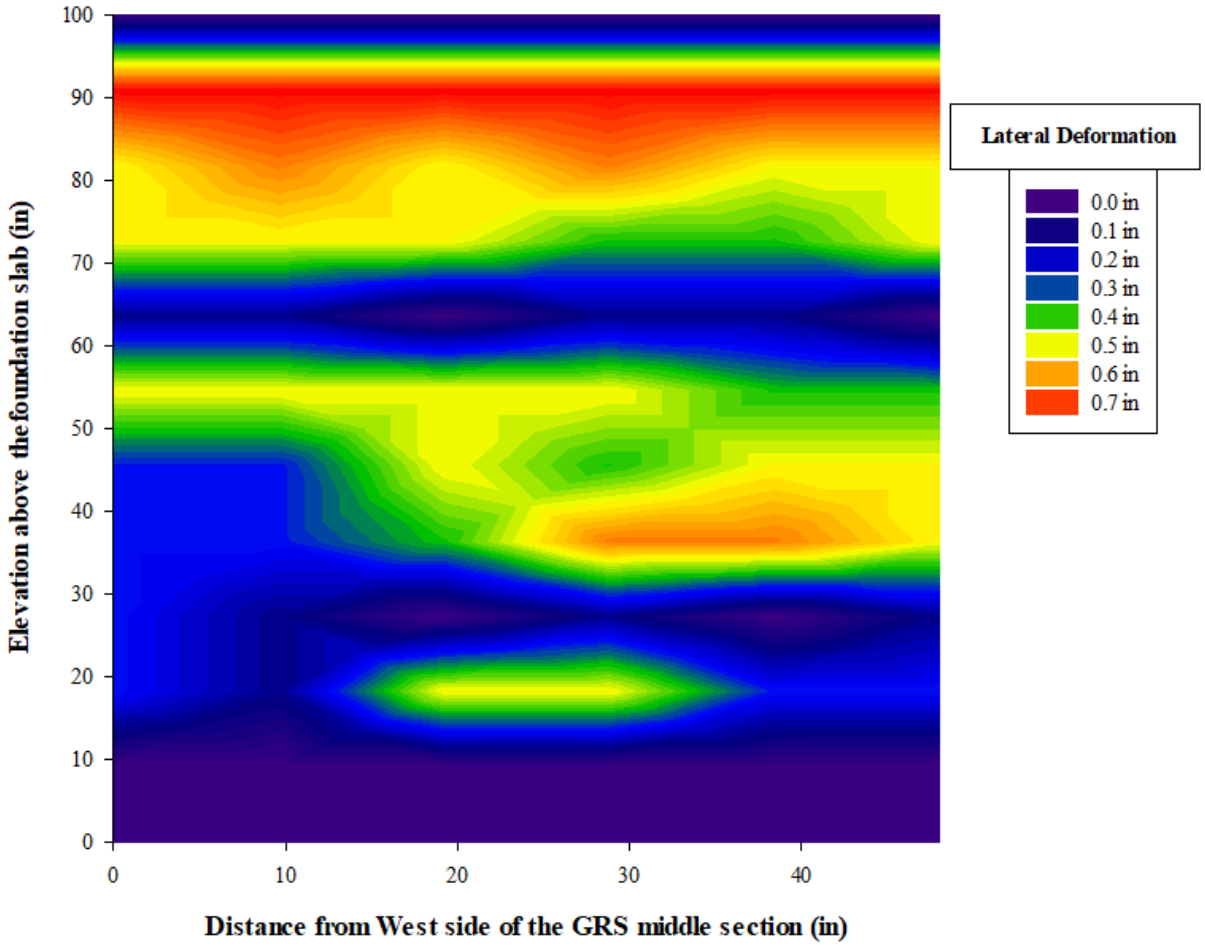

Figure 29 – Contour map of the facing displacement at the end of construction

The results show that the displacement induced by the compaction varies from being negligible to getting close to one full inch. As said in **Chapter 5,** the compaction behind the facing was done no closer than one foot behind it and completed with hand compaction. The variations in displacement could be explained by the fact the operators doing the compaction were changing often, and thus, had different ways of compacting. The bottom layers registered no displacement has they were anchored into a sand bed and it was easier to correct their unwanted displacement. The very top layer did not move as the concrete infilling of the top three layers was already done when the compaction was completed.

6.3.2 During performance test

Figure 30 shows the displacement of the top layer of the facing during the performance tests of Models #1 and #4 through #6.

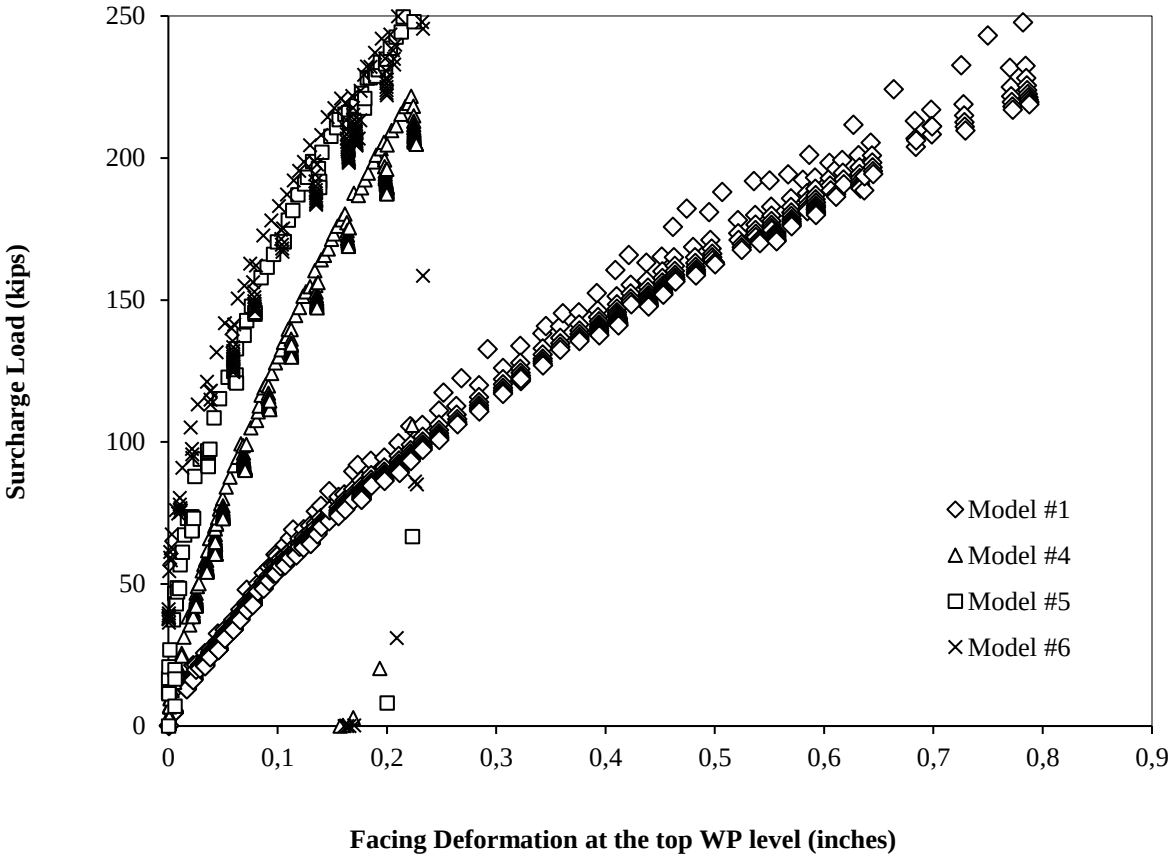

Figure 30 – Facing deformation results at the top WP level during surcharge load testing of GRS Models #1 and #4 through #6. Deformation values shown are mean values from two WPs at the same elevation

Results in **Figure 30** show the importance of adequate compaction in controlling the later deformation of GRS abutments. All models whose results are shown in those figures were built with CMU blocks. As seen from those results, increased compaction effort in Models #4 and #5 resulted in significantly smaller lateral deformations in these models (e.g. 0.19 in. and 0.14 in.,

respectively at 200 kips of surcharge load) as compared to that in the control model (i.e. 0.63 in. at 200 kips in Model #1). Judging by those results, it seems that increasing the compaction effort can yield some interesting improvement in performances in terms of lateral displacement of the structure. Once again, there is no apparent performance variation between Models #4 and #6 despite them using different fill types.

Figure 31 show the facing deformation at different phase of the test and at different elevations on the facing of the GRS Models.

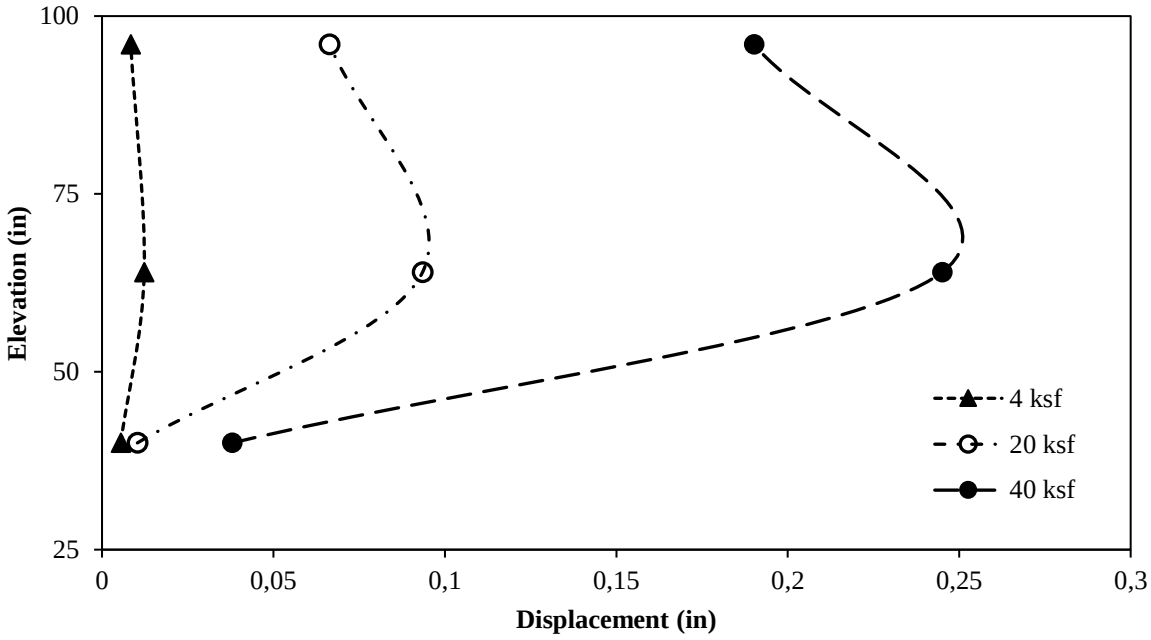

(a)

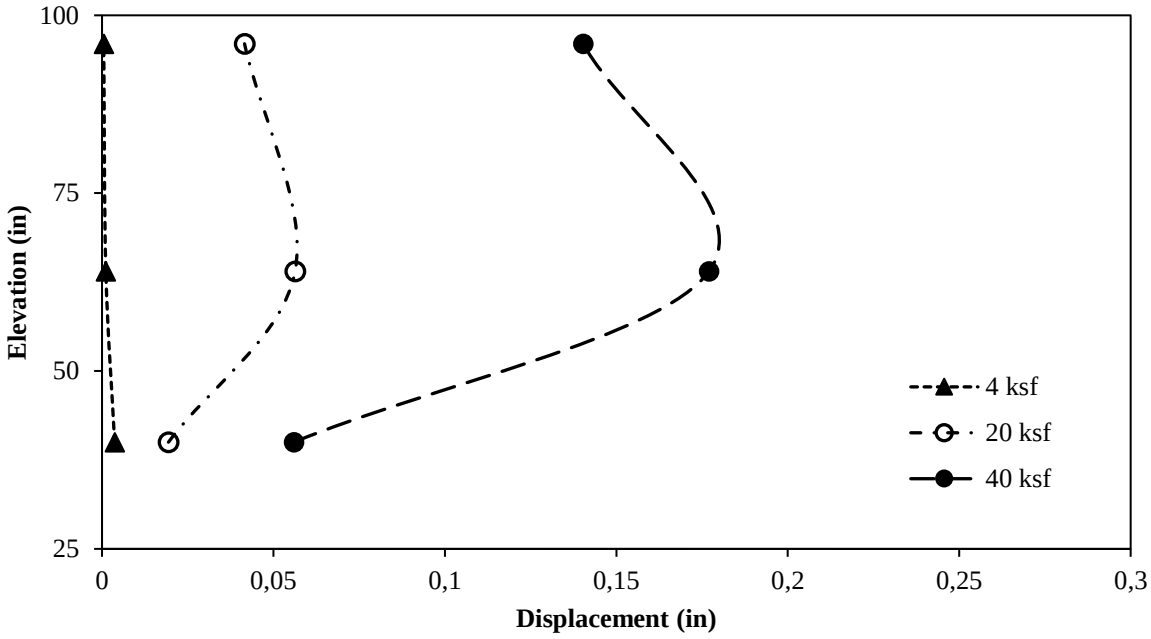

(b)

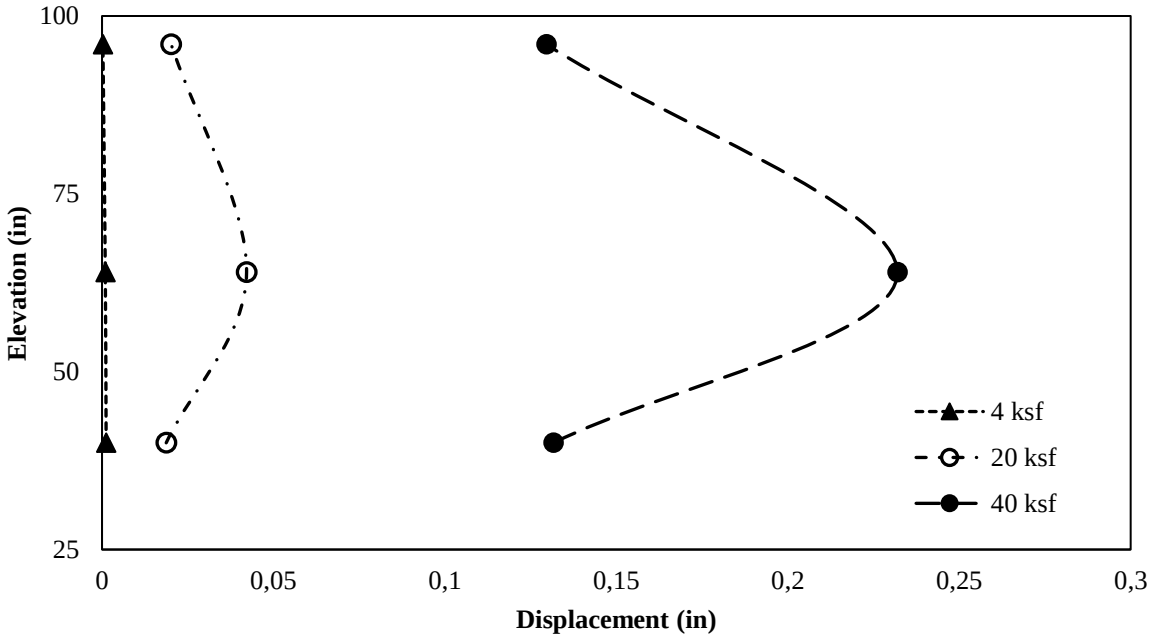

(c)

Figure 31 – Facing deformation at different load levels: (a) Model #4, (b) Model #5, (c) Model #6

As seen from the graphs in **Figure 31**, the facing displacement for all three Models is negligible at the recommended service load level of 4 ksf in FHWA guidelines. When 20 ksf are applied, the facing displacement is still lower than 0.1 in. When 40 ksf are applied, the displacement greatly increases relative to the two previous load phases but is still contained within 0.3 inches. It can also be observed that the maximum displacement is not at the top of the abutment but in the third quarter of it. This could be explained by the fact that it is in this area that a failure would first occur due to a wedge of fill being pushed outwards.

6.4 Reinforcement deformation

Both abutment Models #4 and #6 were instrumented with embedded WPs measuring the deformation of the geotextile reinforcements. **Figures 32 and 33** show the deformation of the geotextile reinforcements at the End of Construction (EoC) and at different loading phases. **Figure 34** show those same deformations compared between Models #4 and #6.

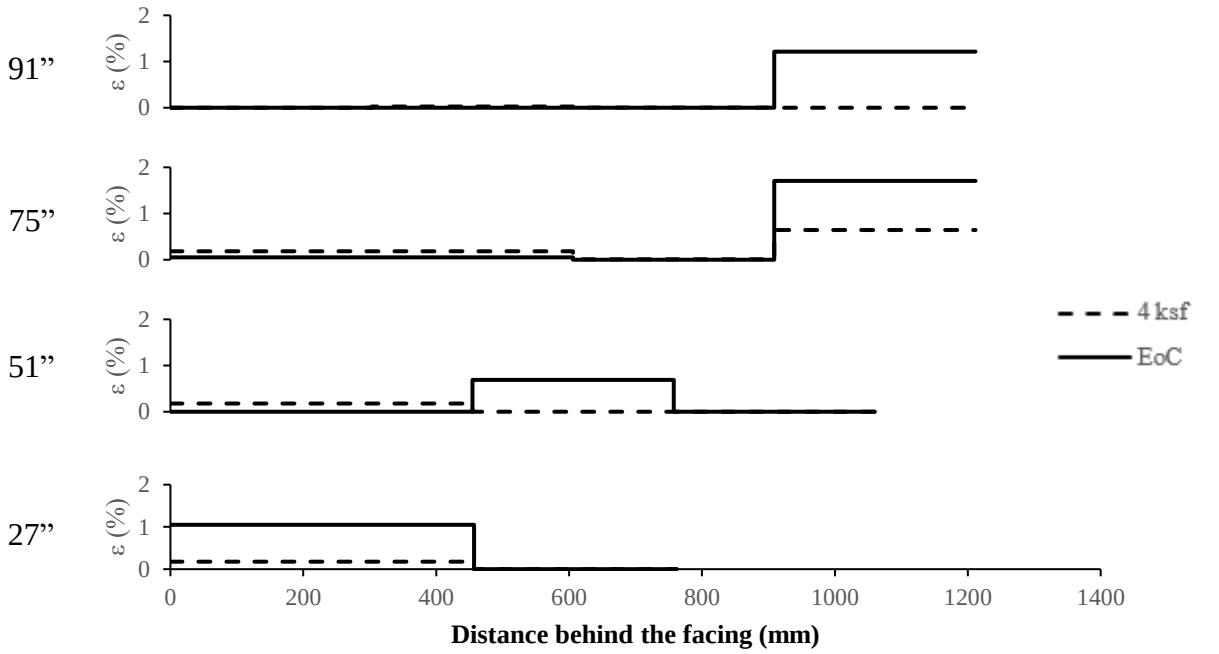

(a)

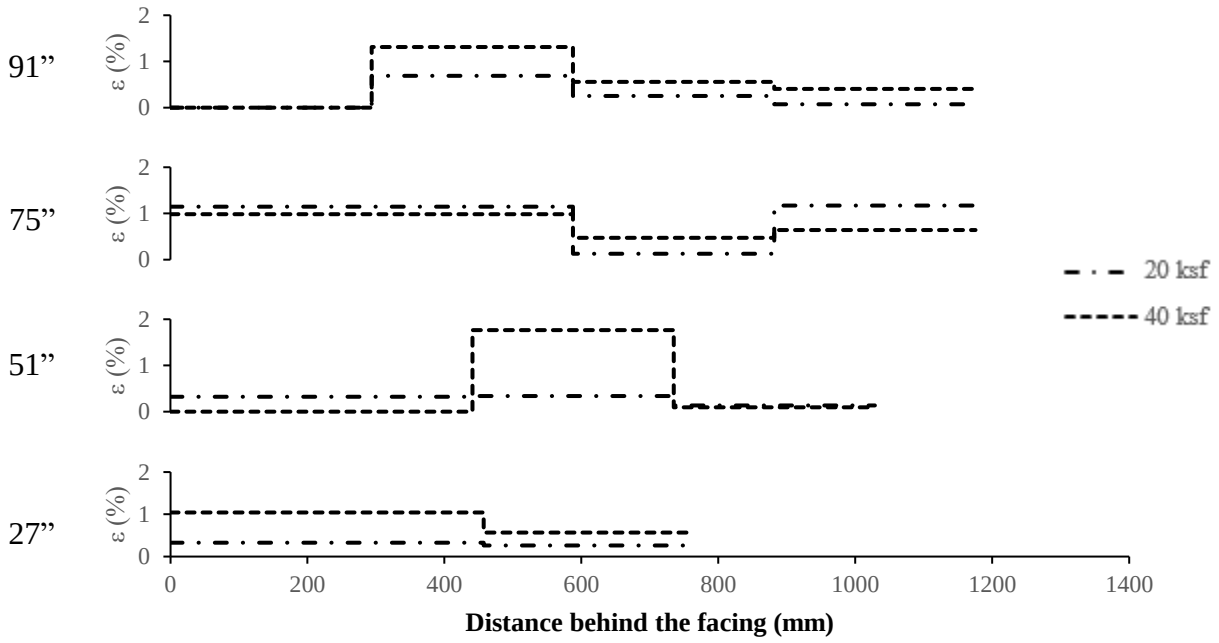

(b)

Figure 32 – Reinforcement strains in abutment model Models #4, (a) EoC and 4 ksf, (b) 20 and 40 ksf

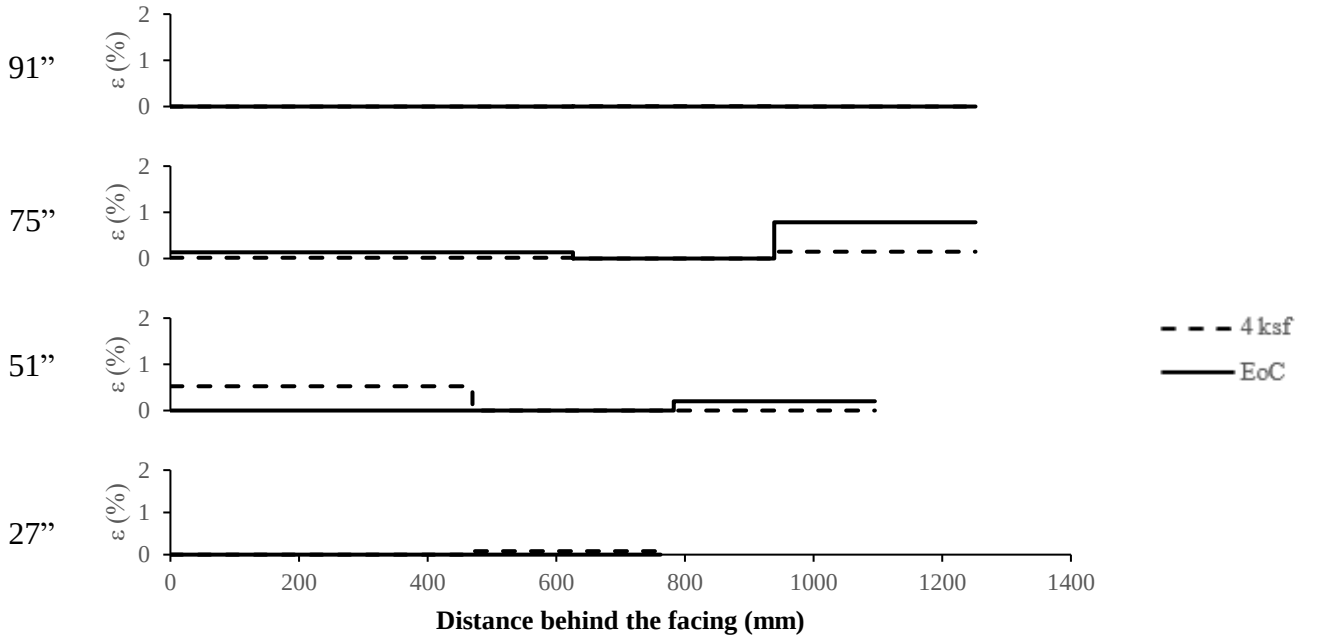

(a)

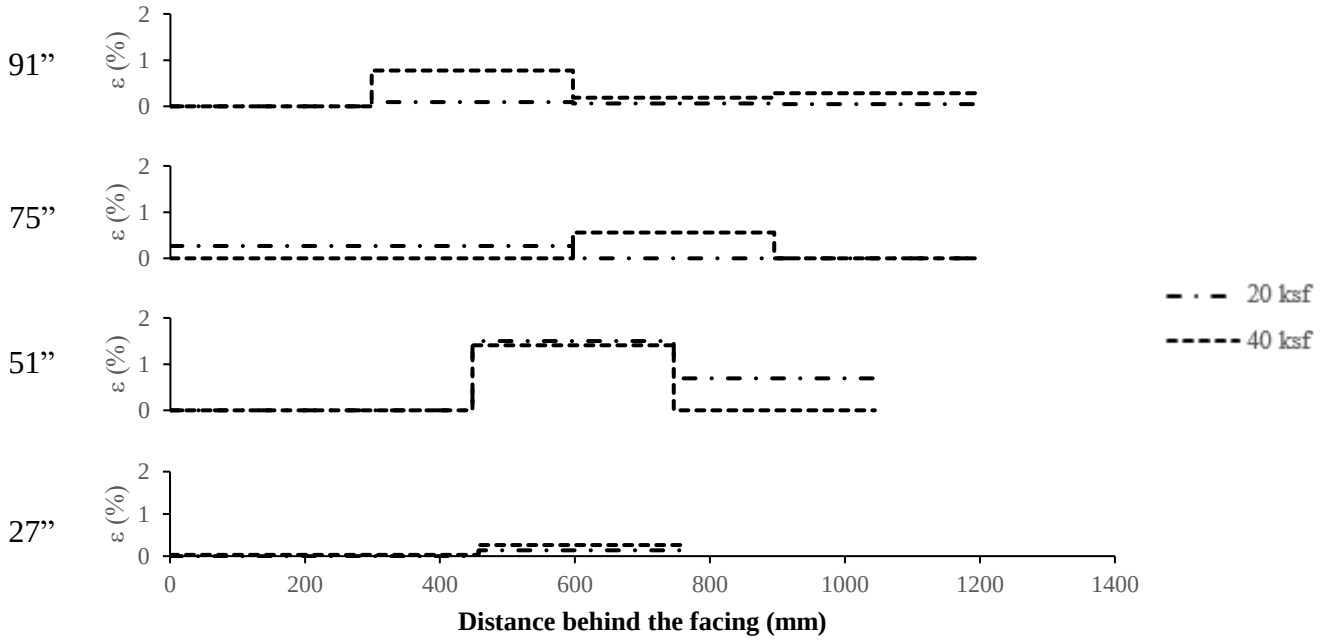

(b)

Figure 33 – Reinforcement deformation of abutment model Models #6, (a) EoC and 4 ksf, (b) 20 and 40 ksf

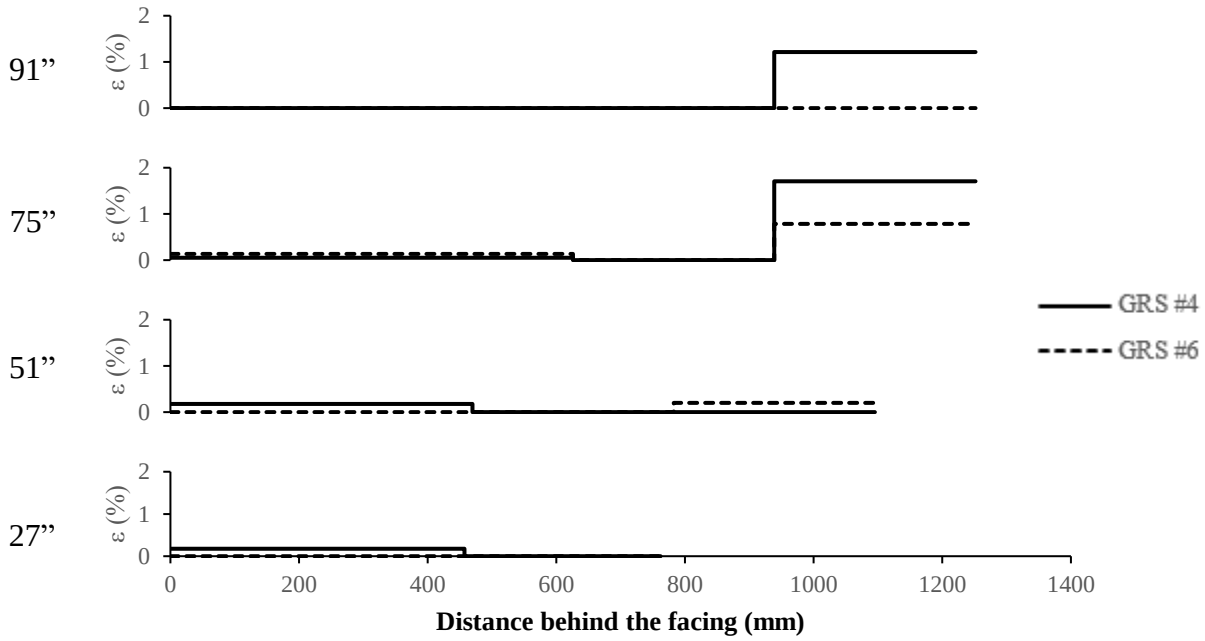
91”
75”
51”
27”
ε (%)
0
1
2
0
200
400
600
800
1000
1200
1400
Distance behind the facing (mm)
GRS #4
GRS #6

(a)

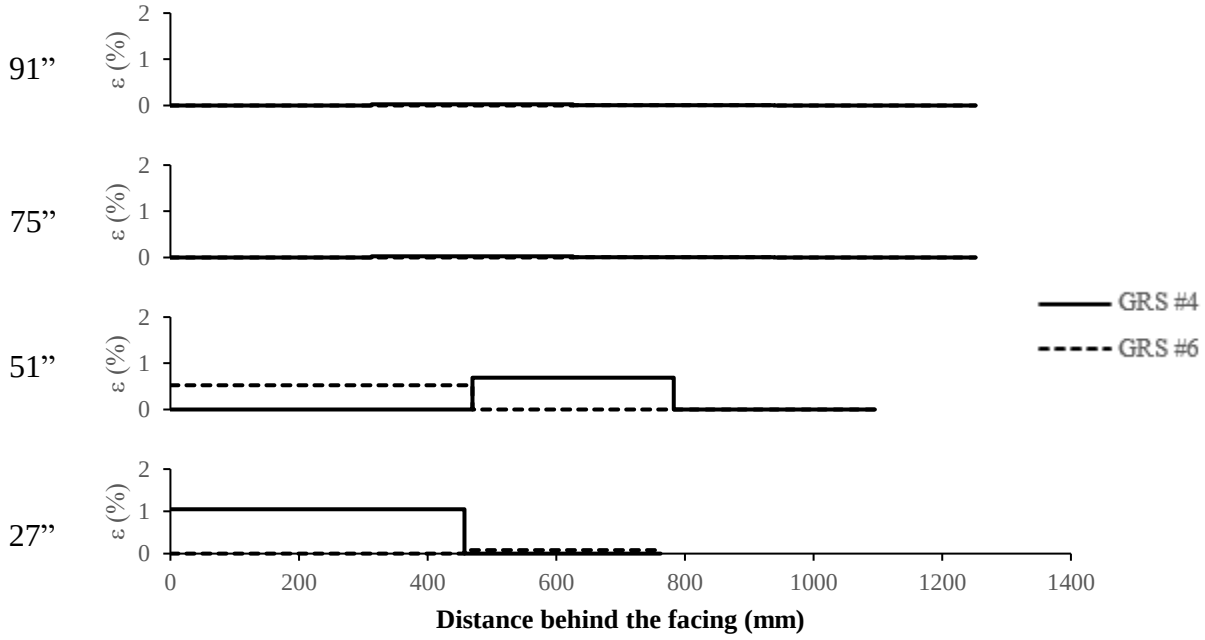
91”
75”
51”
27”
ε (%)
0
1
2
0
200
400
600
800
1000
1200
1400
Distance behind the facing (mm)
GRS #4
GRS #6

(b)

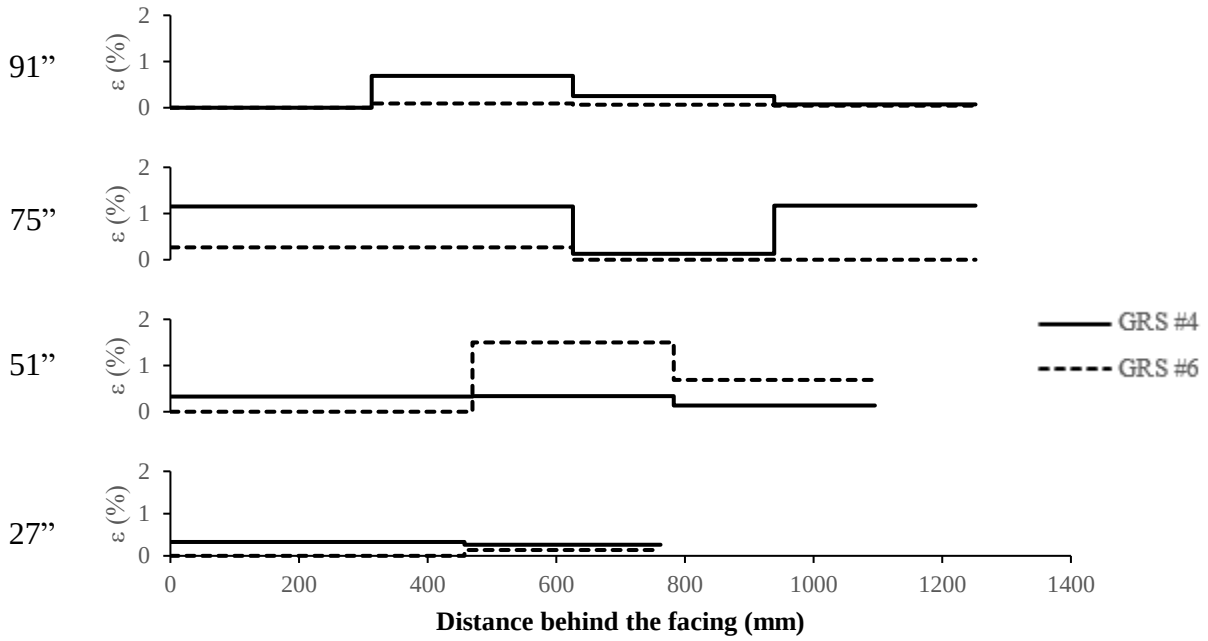

(c)

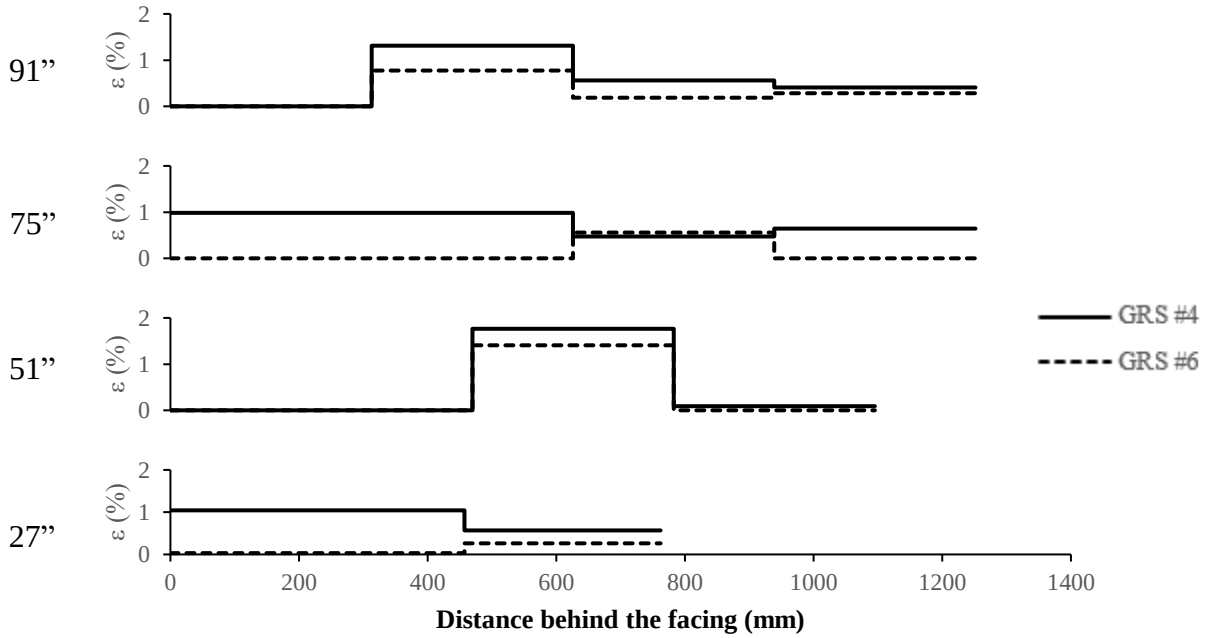

(d)

Figure 34 – Comparison of reinforcement deformation of abutment Models #4 and #6, (a) EoC, (b) 4 ksf, (c) 20 ksf, (d) 40 ksf

Results in **Figures 32 through 34** show that the reinforcement strains become more significant only after the surcharge load reaches or exceeds 20 ksf. However, the distribution of reinforcement strains over the depth of the model abutments do not seem to point to a clear slip plane in the GRS fill.

Using the stress-strain relationship for this geotextile, the maximum amount of stress that the geotextile had to endure can be determined. **Figure 35** shows the maximum strain that each layer had at a certain loading phase.

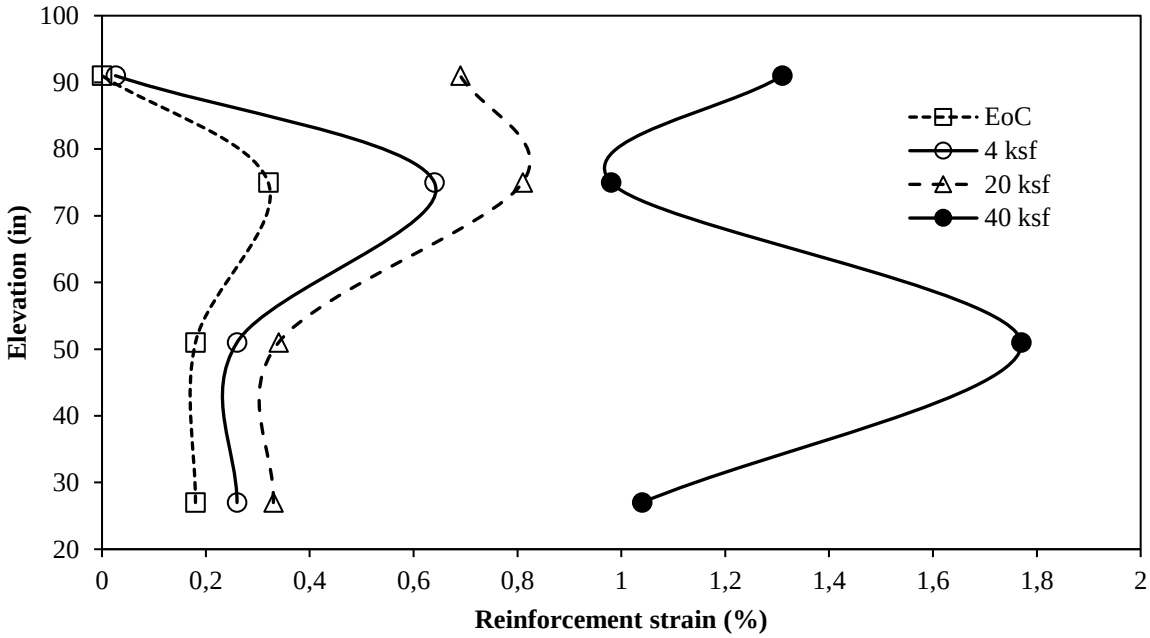

(a)

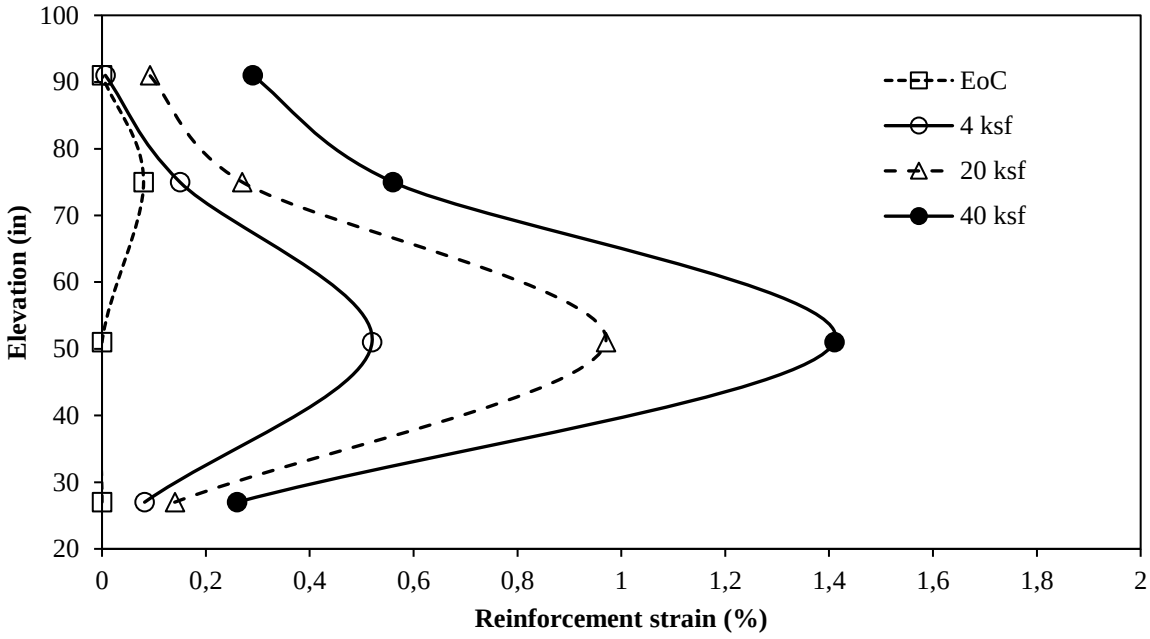

(b)

Figure 35 – Maximum reinforcement strain at different load levels: (a) Model #4, (b) Model #6

Those graphs show that in both models, the geotextile does not exceed 2% of strain, even at 40 ksf of surcharge. Also, the maximum strain does not occur at the top of the structure but rather in the middle of it. This corresponds with the facing deformation results showing that the maximum lateral displacement was situated at an elevation of about 55 inches.

Figure 36 shows the stress-strain curve for Mirafi HP570 geotextile in the cross-machine direction (Cuelo et al 2004). The 0.03%/min corresponds to the strain rate at which the performance testing was done on the GRS models.

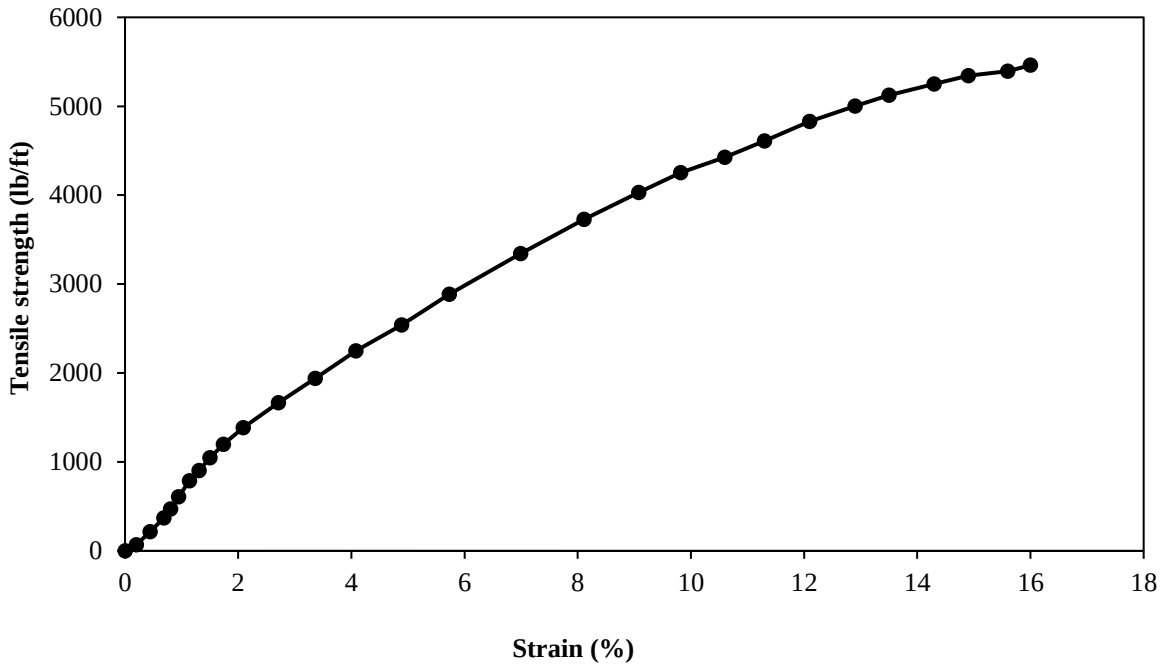

Figure 36 – Load-Strain curve for Mirafi HP570 woven geotextile in the cross-machine direction (XD) at 0.03%/minute strain rate (Cuelho et al. 2004)

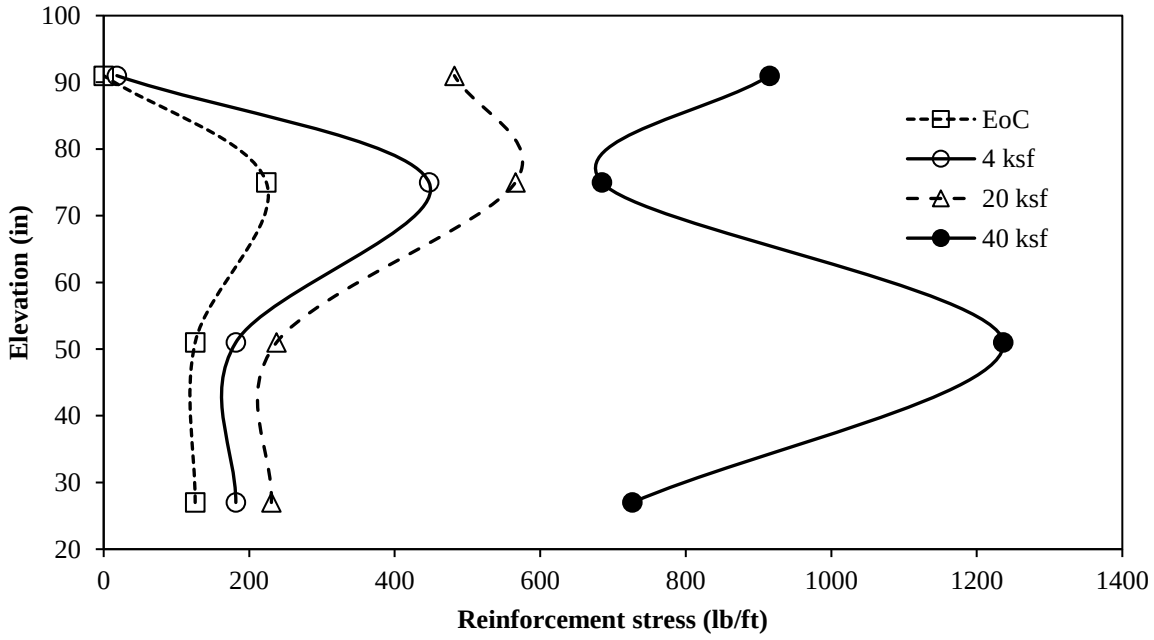

(a)

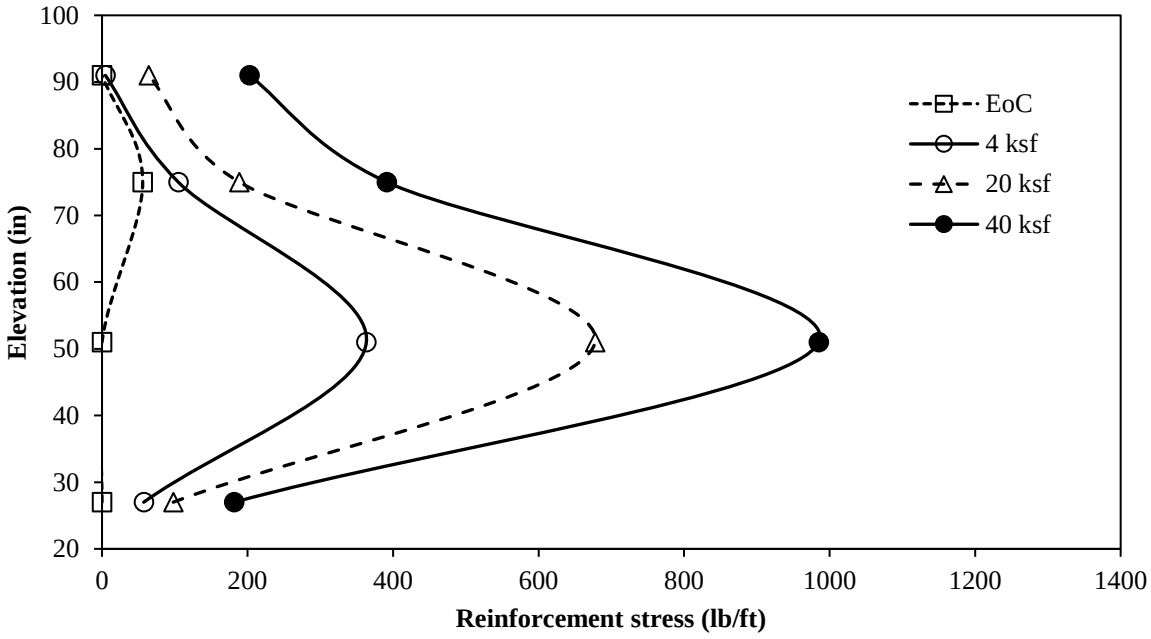

(b)

Figure 37 – Maximum reinforcement stress at different load levels: (a) Model #4, (b) Model #6

Using the stress-strain curve, **Figure 37** shows the determined maximum stress that the reinforcements had to withstand during the loading phases. Since the curve is roughly linear from 0% strain to 2%, the resulting graphs follow the same trend as the ones done for the reinforcement strain. Once again, the maximum reinforcement strain is contained at the halfway height of the structure with values of about 1236 lb/ft and 986 lb/ft for Models #4 and #6 respectively. With Model #6 having lower values, it could be that the dense graded aggregate managed to withstand more pressure and deform less vertically, reducing the stress on the reinforcement layers.

6.5 Construction time and labor requirements

Figure 38 shows a comparison of cumulative construction times in person-hours for the Models #1 and Models #4 through #6.

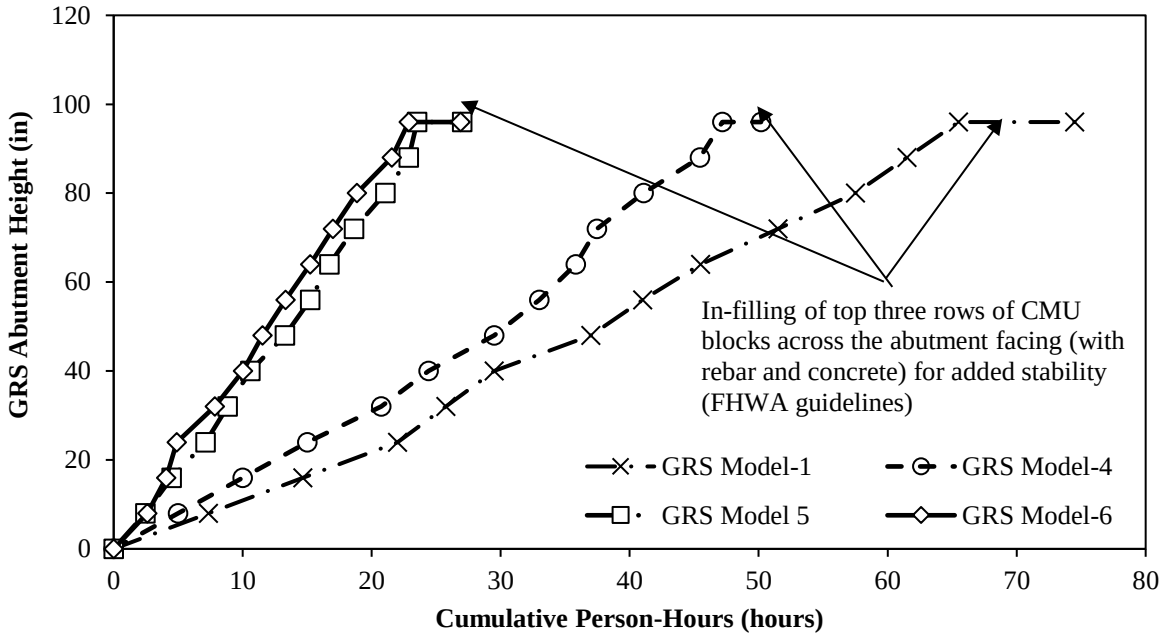

Figure 38 – Comparison of construction time (in person-hours) between GRS Abutment Models #1 and #4 through #6 (Hatami et al. 2020)

Results show that subsequent models that were nominally identical to the control model were built at increasingly faster rate during the project (i.e. Models #4 and #5 vs. Model #1). This demonstrates in quantitative terms that as the team became more familiar with the construction sequence and procedure for the GRS abutment models, the amount of time needed to build each model abutment became increasingly and consistently shorter than those of the previous models including those built with large blocks and reduced compaction effort. This also constitutes a finding with significant practical implications for counties, cities and other stakeholders indicating that as these entities build more GRS-IBS projects across different states, these systems become even more cost competitive and less disruptive of local traffic over time.

These times could be easily improved on site using more appropriate tools and experienced crew. For the compaction, the use of a conventional plate compactor would ensure a more effective way of compacting the backfill than a jumping jack. The concrete used for the grouting was

manually mixed on top of the GRS models. In real conditions, the concrete would either come from a concrete central ready to be poured or be mixed in a mechanical mixer directly brought on site. Also, workers might be more experienced and prepared for the construction of the structure than us, cutting a considerable amount of ineffective time.

6.6 Unit weight survey

Several sand cone tests were conducted on the last model, GRS#6. This test was not an available option for the previous models as the open graded fill would just let the sand past through it and digging a stable hole would not work. With the dense graded fill used in Model #6 however, the cohesion of the fill appeared to be enough to run the tests. The tests were run during the dismantlement of the model and were conducted conforming to the ASTM D1556.

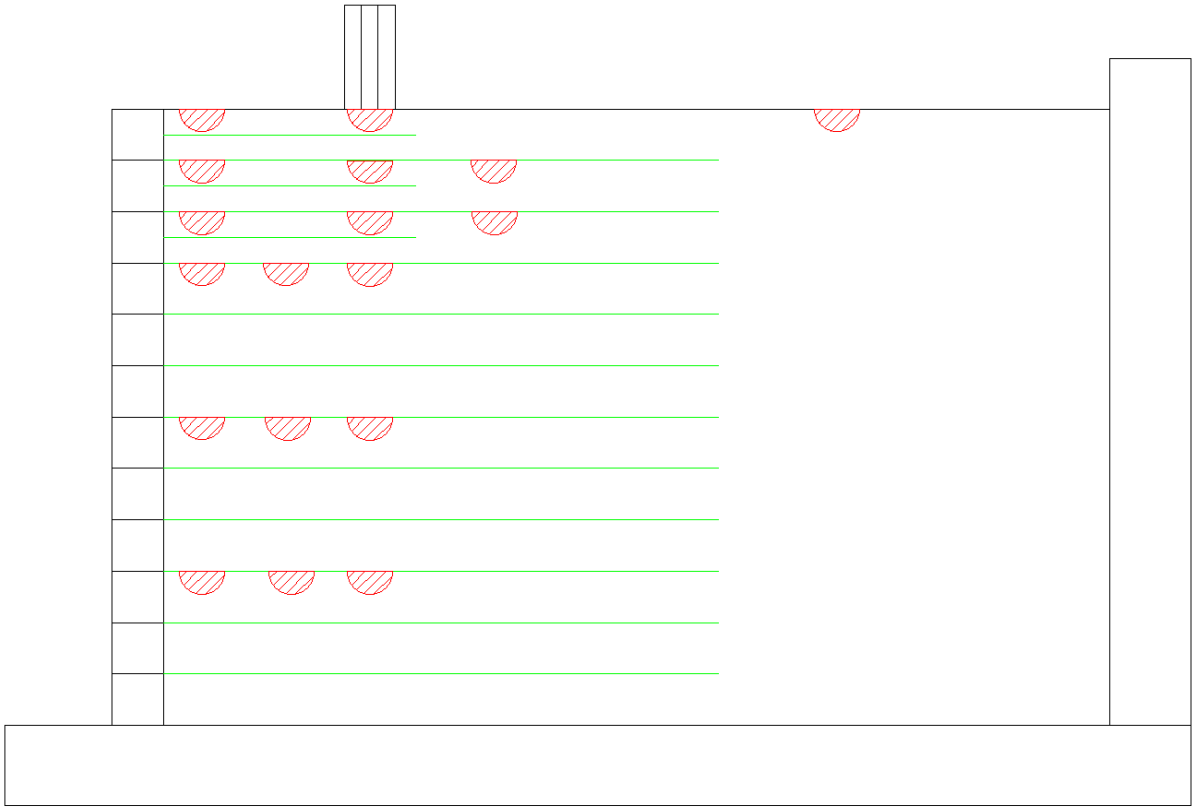

Figure 39 – Position of the different sand cone tests on Model #6

Figure 39 shows the emplacement of the tests. The test positions were chosen as to record the unit weight right behind the facing, under the beam and in a normally compacted area, called "backfill" in the graphs. All the tests were realized in the center section of the GRS. While the in-place unit weight of the fill was taken, the dry unit weight was also determined for each test to make sure values could be easily comparable, as the tests were not all done at the same time.

Figure 40 shows the variation of the in place and dry unit weight of Model #6 after the performance test has been done. The overall trend shown on these diagrams is that the unit weight is going down the closer it gets to the base of the structure. On layer three however, the unit weight value peaks back up. This could be the result of the above layers applying enough pressure for the unit weight to go up again.

Figure 41 shows the variation of the water content of the fill of the GRS#6. Even though all the tests were not done at the same time, it seems that the dense gravel ODOT Type A retained the water coming down from the layers above.

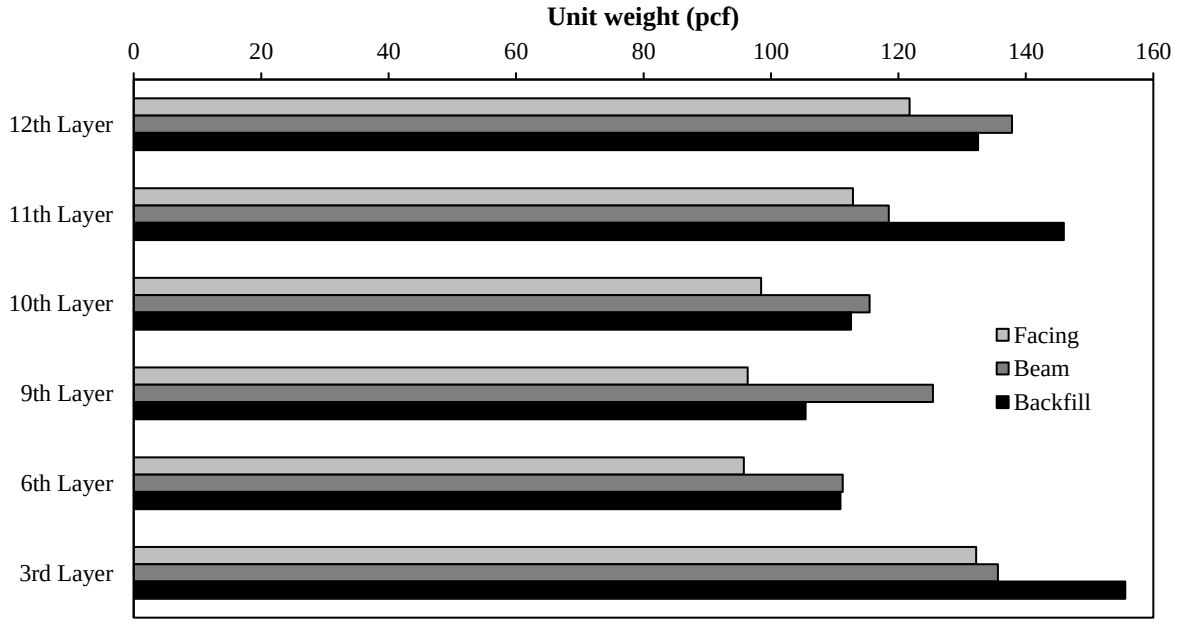

(a)

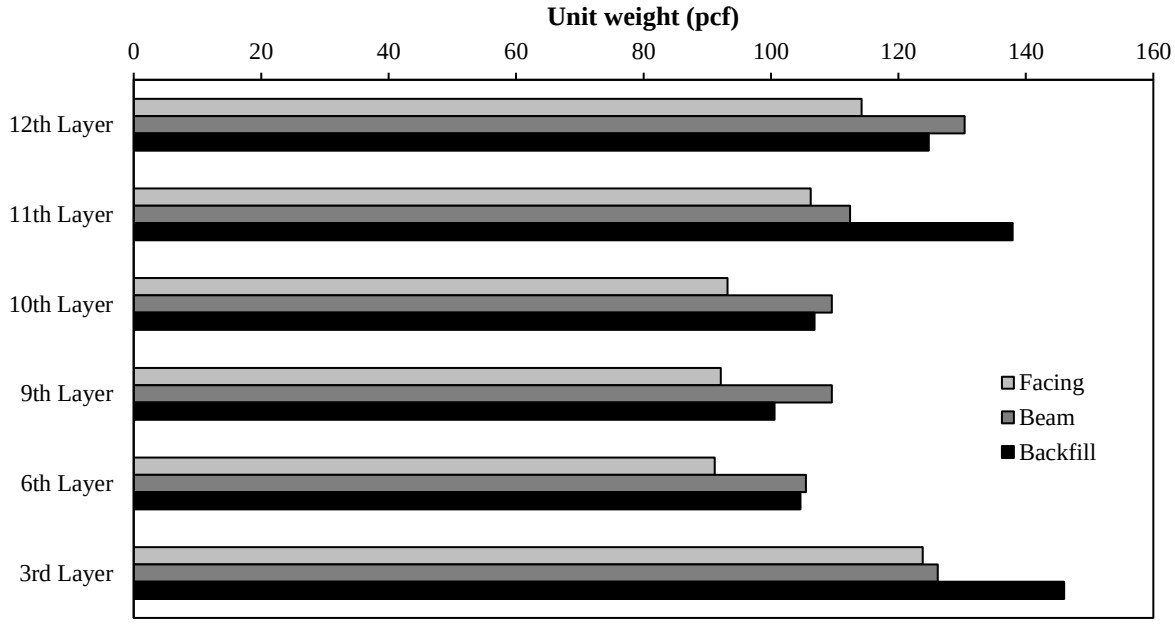

(b)

Figure 40 – Unit weight of the fill of abutment Model #6 after performance testing: (a) in-place unit weight, (b) dry unit weight

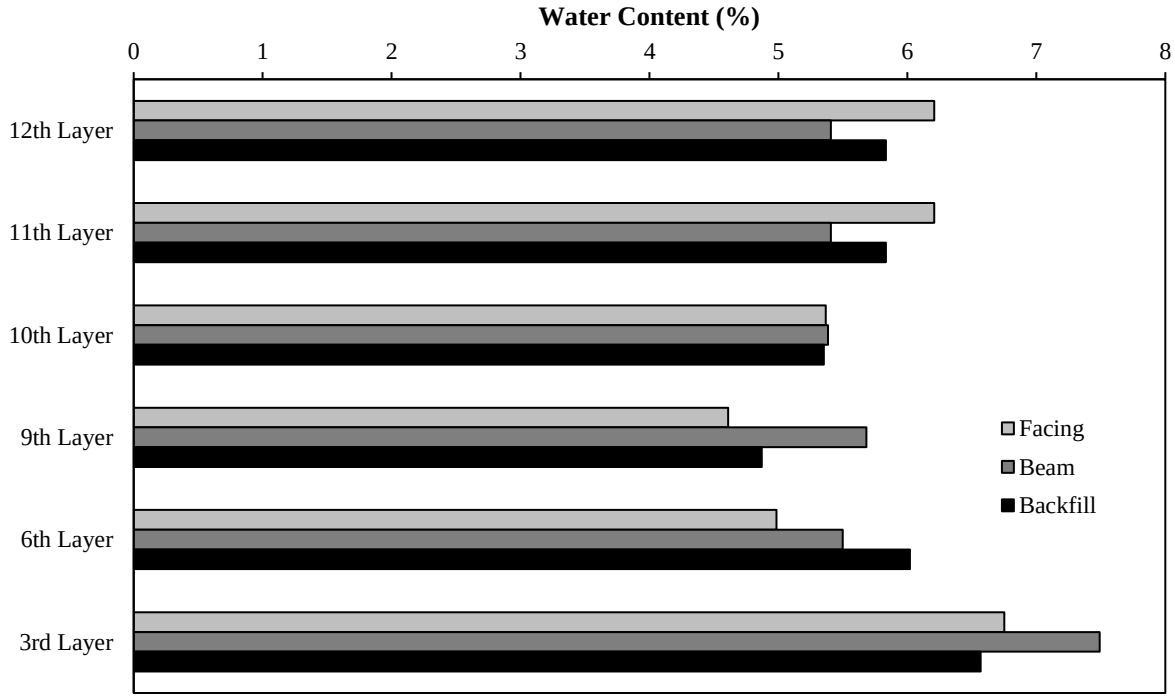

Figure 41 – Water content of the fill of abutment Model #6 after performance testing

The unit weights also vary given their planar locations. Generally, the unit weight is the highest right under the loading area, as the surcharge pressure applied compressed the soil even more. The lowest unit weight values are found behind the facing. As said earlier, the fill right next to the facing was hard to properly compact without disturbing the CMU blocks placements. Additionally to the low compaction, the facing did move outwards a bit during the testing phase, lowering the perceived unit weight even more. The “backfill” area unit weight values are rightfully comprised between the two others.

Compared to the values determined when doing the relative density test, the in-place and dry values are higher. The jumping jack and surcharge loading applied a pressure that cannot be replicated by hand, when doing the laboratory test. These values are also different because of several other factors. Because the sand cone tests were realized on a fill being a mix of smaller and bigger particles, some inaccuracies were expected. When digging the hole, the surface of the hole would not be completely smooth, and the sand would not be able to reach and fill every void. This would result in an overestimation of the soil unit weight since more material has been extracted than the volume determined by the sand.

6.7 Vertical earth pressure

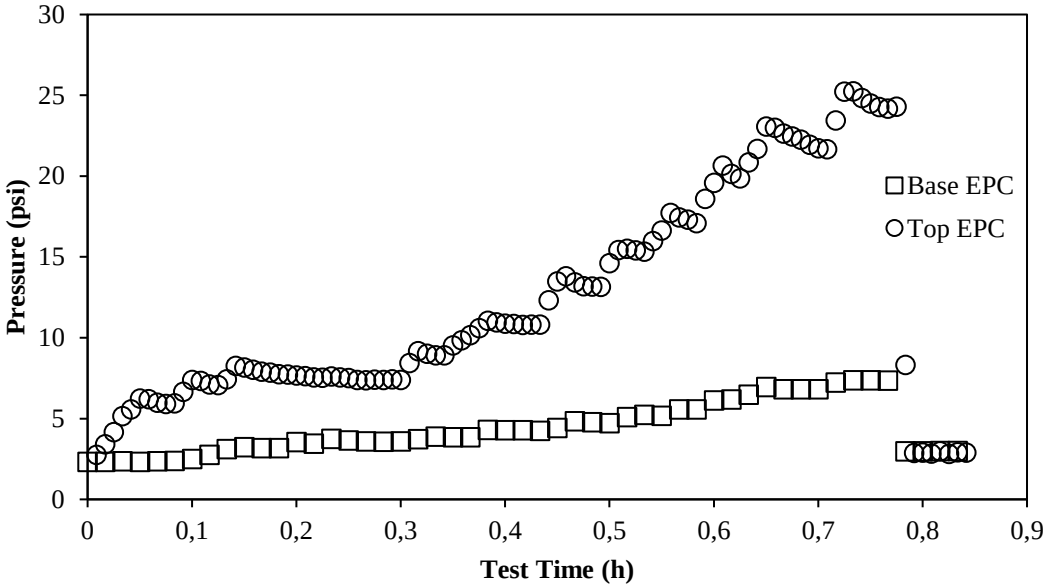

Figure 42 – Vertical earth pressure recorded by EPCs in Model #4 during the performance test

Figure 42 shows the evolution of the vertical earth pressure inside Model #4. Because of complications, only those two EPCs were able to properly function and record useful data during the testing. Other EPCs data were found to inconclusive. The top EPC data shown here is from the one at an elevation of 47 inches inside the GRS fill while the base one is the one placed on the left side under the facing.

As shown by this graph, the vertical pressure that reaches the base of model is dissipated as the pressure does not go above 8 psi. On the other end, the top EPC recorded pressure more than three times higher (~25 psi) than what the base was recording. This is mostly because this EPC is placed higher and centered relative to the application point of the load.

Chapter 7 – CONCLUSION AND RECOMMENDATION FOR FUTURE WORK

7.1 Summary and Conclusions

In this study, the main objective of building three new GRS abutment models similar to the control model GRS#1 was completed. Those were built in an attempted to fill the undocumented gap about the influence of the compaction of the fill on the performances of the GRS abutment structures.

While not as critical as the main objective, the ancillary testing allowed for a deeper understanding of the different materials used to build those structures.

During the construction of the models, the preparation and embedment of the instrumentation was a crucial process as it would directly impact on the ability to gather useful data and analyze it later. The instrumentation process would however greatly increase the time needed to build a model, as opposed to a model without any instrumentation. From a pure construction standpoint, the dense graded ODOT Type A aggregate brought issues that never appeared with the use of the open graded #2 Cover aggregate. These issues were mainly related to the poor workability of the material coupled with its sensitive behavior when its moisture content fluctuated.

The performance tests of those models showed that an increase in compaction effort was indeed very beneficial for the overall stability of the structure. All three models were able to easily meet the FHWA settlement requirements with factors of safety of at least 11 when reaching the maximum applied surcharge.

The same improvement in performance was noticeable with the facing lateral displacement during testing as the maximum values were all below 0.25 in. Facing deformation monitoring showed that the halfway height of the structure is where the lateral deformation is the highest.

Monitoring of the reinforcement deformation revealed that the geotextile did not strain above 2% despite having surcharges as high as 40 ksf. This resulted in the reinforcement having to withstand stresses of no more than 1236 lb/ft during the testing phases, far away from its ultimate strength.

The unit weight survey was also one of the main objectives of this study, and while the conditions weren't perfect for the use of a sand cone apparatus, it still managed to bring some useful information on how the compaction of the fill would vary given the area. Given the numerical values obtained, the dense graded gravel was overall well compacted. The back of the facing was however less compacted because of the difficulty to do it without disturbing the facing.

In the end, a higher compaction of the fill allowed the GRS abutments to gain significant performance improvement over their lower compaction counterpart. And while this performance gain was noticeable in a lot of important performance areas, the utilization of a denser fill did not change the results in a way that would make it worth it to use it, as its workability is worse than that of the open graded one.

7.2 Recommendation for Future Work

The following recommendation are made for future work in continuation of this study:

1. While a lot of combinations can be made with the GRS abutment models by changing the properties of the key components, the next plausible combination would be to use the large concrete blocks (2' × 2' × 4') as facing. This would then be coupled with the open graded gravel, three passes of compaction and reinforcement spacing of 12 in. Results would then be compared to that of GRS abutment models GRS #2 and GRS #3.

2. A test bed similar to the one done with the #2 Cover aggregate needs to be done with the ODOT Type A. The results would then need to be compared between the two aggregates, but also to the values found while doing the unit weight survey.
3. Some additional DST tests would need to be done for both aggregates used. As seen from the data contained in this study, some of the DST results would sometime greatly deviate from the expected behavior. Redoing some of those and adding some more tests would help in obtaining more accurate values for the friction angles of the aggregates.
4. Something also needs to be done about the EPCs as they are having trouble staying in working order until the end of the test, sometime even stopping before the test even begins. There is most likely a sensible spot where the cables connect with the actual EPC. Maybe an idea would be to enclose this sensible area with something akin to a hard shell. The use of rigid enough tubes may also work.
5. Numerical modeling the GRS model would be quite useful for potential future projects. With now six different already tested models and several component characteristics already known, the modeling could be calibrated with actual data rather than just assumptions.

References

1. Abu-Farsakh, M., Ardah, A. and Voyiadjis, G., 2018, "3D Finite element analysis of the geosynthetic reinforced soil-integrated bridge system (GRS-IBS) under different loading conditions", *Transportation Geotechnics*, Elsevier, No. 15, pp. 70-83.

2. Adams, M., Nicks, J., Stabile, T., Wu, J., Schlatter, W., and Hartmann, J., 2011a., "Geosynthetic Reinforced Soil Integrated Bridge System Interim Implementation Guide", *Report No. FHWA-HRT-11-026*, Federal Highway Administration, Washington, DC. Available at: http://www.fhwa.dot.gov/publications/research/infrastructure/structures/11026/index.cfm

3. Adams, M., Nicks, J., Stabile, T., Wu, J., Schlatter, W., and Hartmann, J., 2011b., "Geosynthetic Reinforced Soil Integrated Bridge System Synthesis Report", *Report No. FHWA-HRT-11-027*, Federal Highway Administration, Washington, DC.

4. Adams, M. and Nicks, J., 2018. Design and Construction Guidelines for Geosynthetic Reinforced Soil Abutments and Integrated Bridge Systems, *Report No. FHWA-HRT-17-080*, Federal Highway Administration, Washington, DC.

5. ASTM C136 / C136M-14, Standard Test Method for Sieve Analysis of Fine and Coarse Aggregates, ASTM International, West Conshohocken, PA, 2014, www.astm.org.

6. ASTM D1556 / D1556M-15e1, Standard Test Method for Density and Unit Weight of Soil in Place by Sand-Cone Method, ASTM International, West Conshohocken, PA, 2015, www.astm.org.

7. ASTM D3080 / D3080M-11, Standard Test Method for Direct Shear Test of Soils under Consolidated Drained Conditions, ASTM International, West Conshohocken, PA, 2011, www.astm.org.

8. ASTM D4253-16e1, Standard Test Methods for Maximum Index Density and Unit Weight of Soils Using a Vibratory Table, ASTM International, West Conshohocken, PA, 2016, www.astm.org.

9. Budge, A.S., Dasenbrock, D.D., Mattison, D.J., Bryant, G.K., Grosser, A.T., Adams, M. and Nicks, J., 2014, "Instrumentation and Early Performance of a Large Grade GRS-IBS Wall", *Geotechnical Special Publications*, ASCE, No. 234, pp. 4213-4227.

10. Chicago Pneumatic, 2011. Safety and operating instructions for Rammer MS 780, https://www.crowderpneumatics.com/assets/files/MS%20780%20Tamper%20Safety%20&%20Operating%20Instructions.pdf.

11. Cuelho E., Ganeshan S. 2004. “Developing test protocols to determine geosynthetic material properties that better represent traffic loading conditions.” *Western Transportation Institute College of Engineering*, Montana State University - Bozeman, Final Report.

12. Christopher, B. R., Stulgis, R. P., 2005, “Low Permeable Backfill Soils in Geosynthetic Reinforced Soil Walls: State-of-the-Practice in North America”, *Cooperative Conference Proceedings*, NAGS/GRI-19.

13. Doger R, 2020. “Influence of Facing on the Construction and Structural Performance of GRS Bridge Abutments”, PhD Dissertation, CEES, University of Oklahoma, Norman, OK, USA.

14. Doger, R., Hatami, K., Sheffert S., Simpson, T., Boutin, J., Schnabel, S. and Falcon, K., 2019, “Accelerated Bridge Construction using Large-Block GRS Abutments”. Poster resented at: SPTC summer symposium Poster 2019.

15. Esmaili, D., Hatami, K., 2015, “Measured Performance and Stability Analysis of Large-Scale Reinforced Model Embankments at Different Moisture Contents”, *International Journal of Geosynthetics and Ground Engineering*, Springer, No. 22, pp 1-22.

16. Han, J., Jiang, Y. and Xu, C., 2017, “Recent advances in geosynthetic-reinforced retaining walls for highway applications”, *Frontiers of Structural and Civil Engineering*, Higher Education and Springer-Verlag, No 12, Vol. 2, pp. 239-247.

17. Hatami K, Doger R, Boutin J, 2020. Feasibility Study of GRS Systems for Bridge Abutments in Oklahoma: Influence of Facing and Aggregate Fill on Performance, *Final Report No. FHWA-OK-19-09, ODOT SP&R ITEM NUMBER 2262*, ODOT, Oklahoma City, OK, January 2020, 43p.

18. Ngo, T., 2016, “Feasibility Study of Geosynthetic Reinforced Soil Integrated Bridge Systems (GRS-IBS) in Oklahoma”, *Master’s Degree Thesis*, University of Oklahoma, Graduate College.

19. Saghebfar, M., Abu-Farsakh, M., Ardah A., Chen, Q. and Fernandez, B. A., 2017, “Performance monitoring of Geosynthetic Reinforced Soil Integrated Bridge System (GRS-IBS) in Louisiana”, *Geotextiles and Geomembranes*, Elsevier, No. 45, pp. 34-47.

20. Tencate Geosynthetics, 2015, Mirafi HP570 Technical Data Sheet, http://www.roadfabrics.com/wp-content/uploads/2015/08/hp570_tds.pdf.

21. Warren, K.A., Whelen, M.J., Hite, J. and Adams, M., 2014, "Three Year Evaluation of Thermally Induced Strain and Corresponding Lateral End Pressures for a GRS IBS in Ohio", *Geotechnical Special Publications*, ASCE, No. 234, pp. 4238-4252.

22. Wu., J. T. H. and Payeur, J-B., 2014, "Connection Stability Analysis of Segmental Geosynthetic Reinforced Soil (GRS) Walls", *Transportation Infrastructure Geotechnology*, Springer, No. 2, pp. 1-17.

23. Xie, Y. and Leshcinsky, B., 2015, "MSE walls as bridge abutments: Optimal reinforcement density", *Geotextiles and Geomembranes*, Elsevier, No. 43, pp. 128-138.

24. Yarivand, A., Behnia, C., Bakhtiyari, S., and Ghalandarzadeh, A., 2016, "Performance of geosynthetic reinforced soil bridge abutments with modular block facing under fire scenarios", *Computers and Geotechnics*, Elsevier, No. 85, pp. 28-40.

25. Zheng, Y. and Fox, P.J., 2017, "Numerical Investigation of the Geosynthetic Reinforced Soil–Integrated Bridge System under Static Loading", *Journal of Geotechnical and Geoenvironmental Engineering*, ASCE, No. 143.